SAND2019-14680C

3D Simulations of Reaction Front Dynamics in a 1:1 Co/Al Reactive Multilayer System

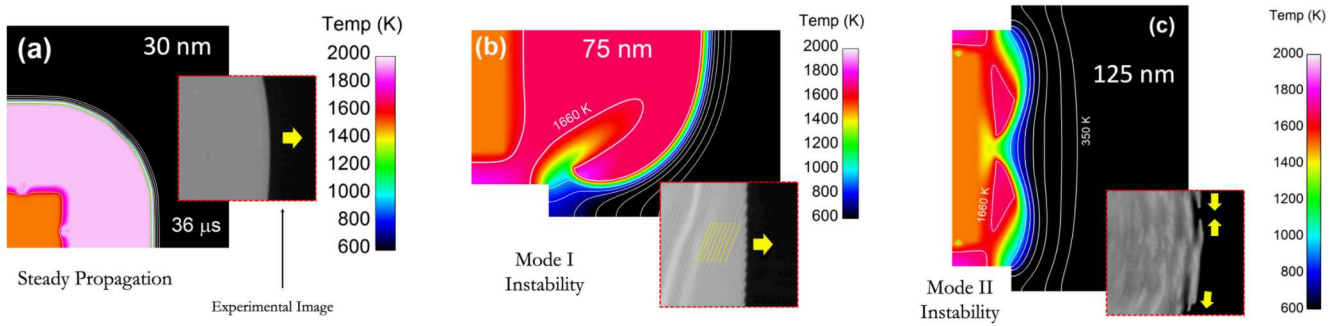

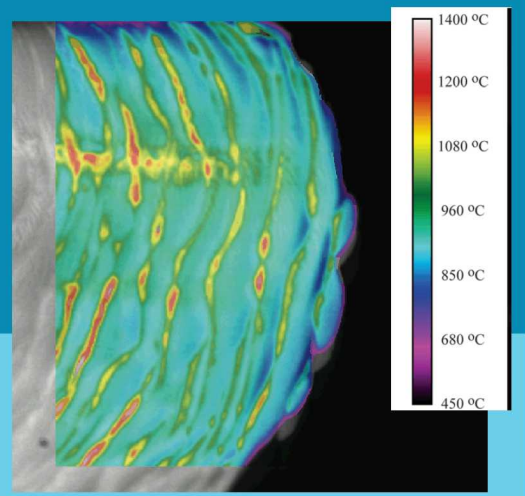

PRESENTED BY

David Kittell, Thursday December 5, 3:30 PM
Co-Authors Michael Abere and David Adams

2019 Materials Research Society Fall Meeting & Exhibit, December 1-6.
Symposium FF06: Advances in the Fundamental Understanding and Functionalization of Reactive Materials

SAND2019-xxxx C, approved for unclassified unlimited release (UUR)

Sandia National Laboratories is a multimission laboratory managed and operated by National Technology & Engineering Solutions of Sandia, LLC, a wholly owned subsidiary of Honeywell International Inc., for the U.S. Department of Energy's National Nuclear Security Administration under contract DE-NA0003525.

Outline for 3D Simulations of Reaction Front Dynamics in Co/Al

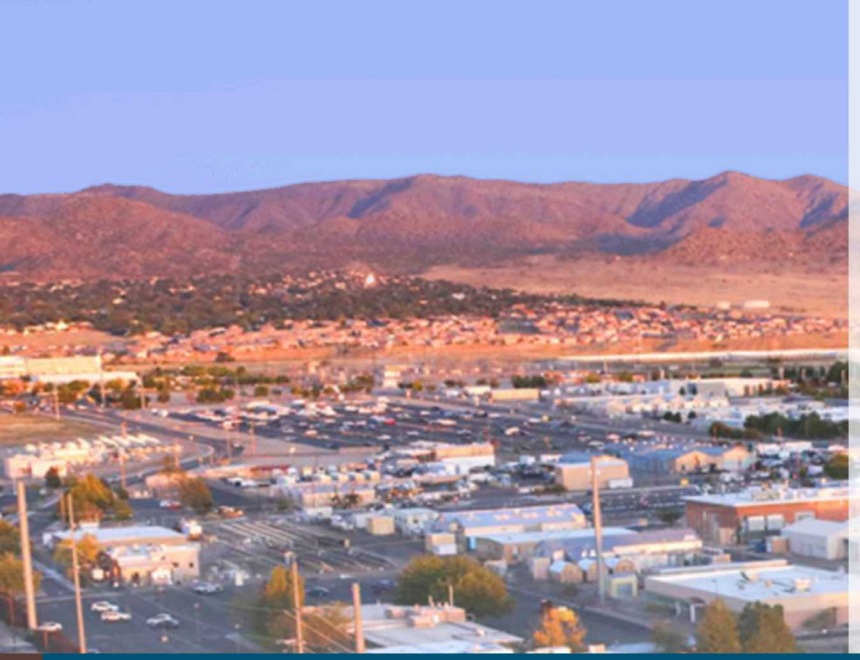

INTRODUCTION

Gasless Reactive Materials

Rapid, self-sustained exothermic reactions that emit light and heat

- Low free energy of the products
- Overcome reaction barriers by physical mixing or by enabling mass diffusion (e.g., increase T)

A large variety of two-component systems (Ni/Ti, Ni/Al, etc…)

- $A + B \Longrightarrow AB$

Self-propagating high-temperature synthesis (SHS) led to reactive multilayers

- Merzhanov ~ 1960's
- Self-propagating crystallization in amorphous films
- Vapor deposition of laminates

Disordered Powder Compacts

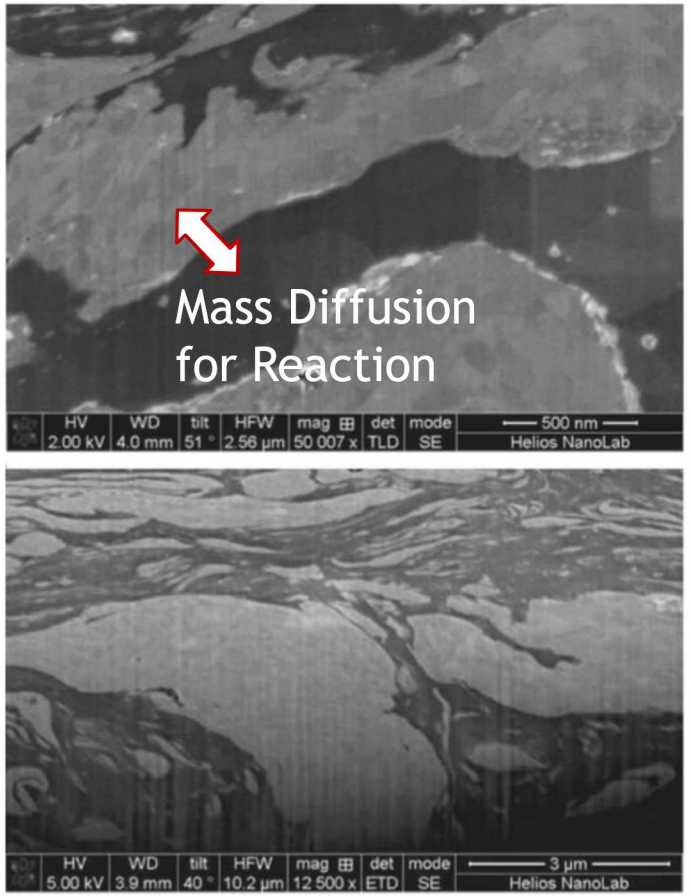

High-energy ball milled (HEBM) Ni/Al powder compact from Reeves *et al.* (2010)

Ordered Multilayers

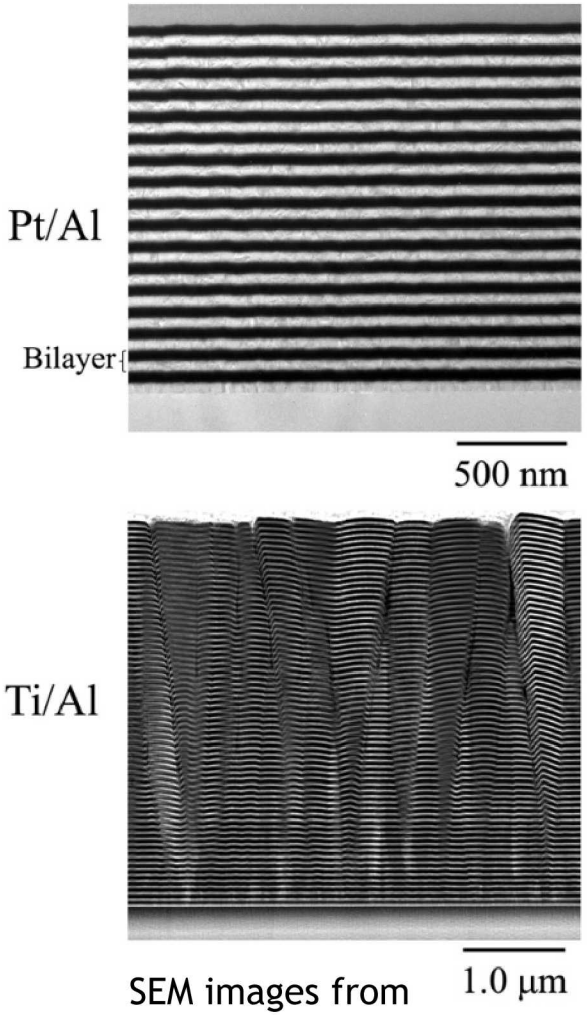

SEM images from Adams (2015)

Combustion Instabilities

1D, 2D, and 3D instabilities are observed in gasless reactive systems - Reeves and Adams (2014)

Spin instabilities are the most commonly observed instability for reactive multilayers

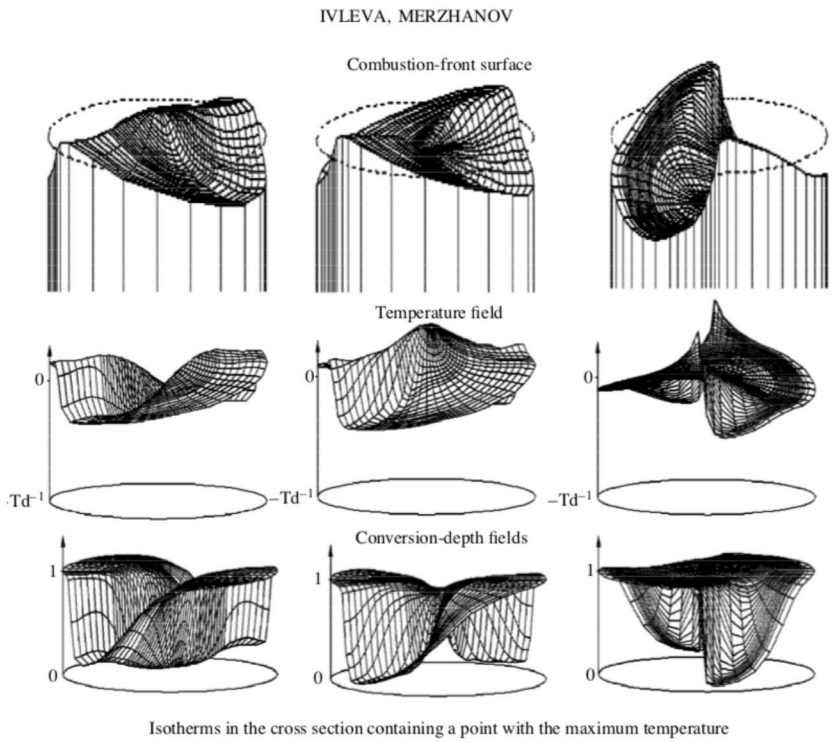

Isotherms in the cross section containing a point with the maximum temperature

- Spin instabilities were first observed during combustion of a Ti cylinder in a N_2 atmosphere by Filonenko and Vershennikov (1975)
- 3D simulations by Ivleva and Merzhanov (2000)

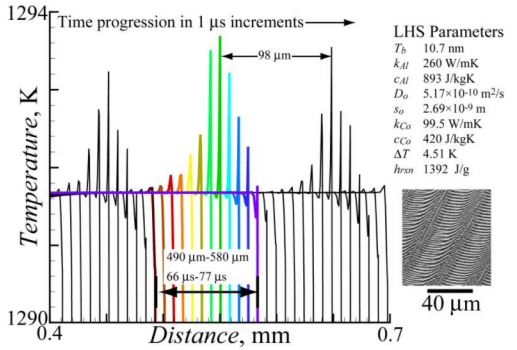

- 1D auto-oscillation in Co/Al multilayers – simulation by Hobbs *et al.* (2008)

- Recent results for Sc/Ag by Adams *et al.* (2019)

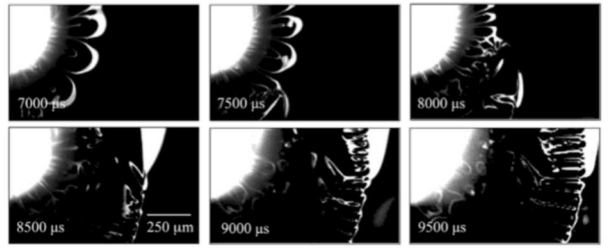

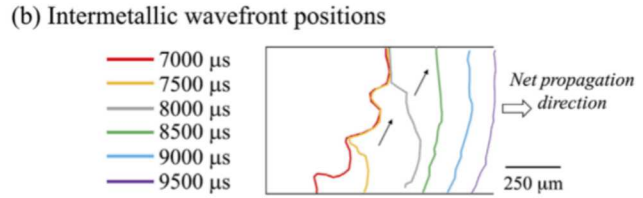

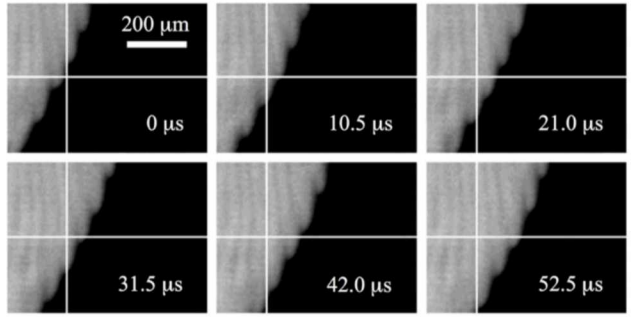

- 2D spin instability in Co/Al multilayers – experimental images from McDonald *et al.* (2009)

Combustion Instabilities, Continued

Spinlike reaction fronts in Co/Al multilayers from Reeves and Adams (2014)

- Observed in free-standing 7.5 μm (total thickness) 1:1 Co/Al reactive multilayers
- Spin band characteristics depend on Co + Al layer (Bilayer) spacing
- Electron-transparent thicknesses, too (Abere *et al.*, this conference)

Undesirable for controlled heat release applications

- Spin band mechanism is relatively unexplored
- Proposed mechanism is shown at top, right

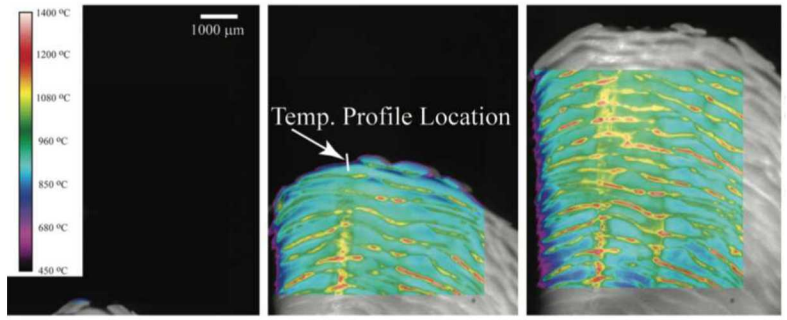

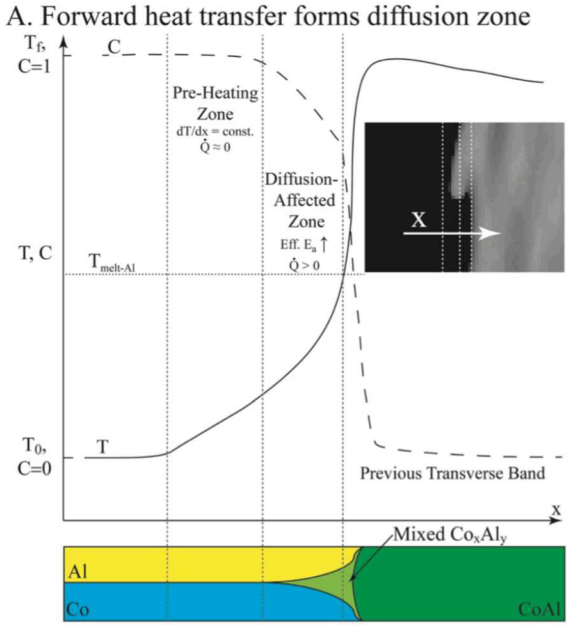

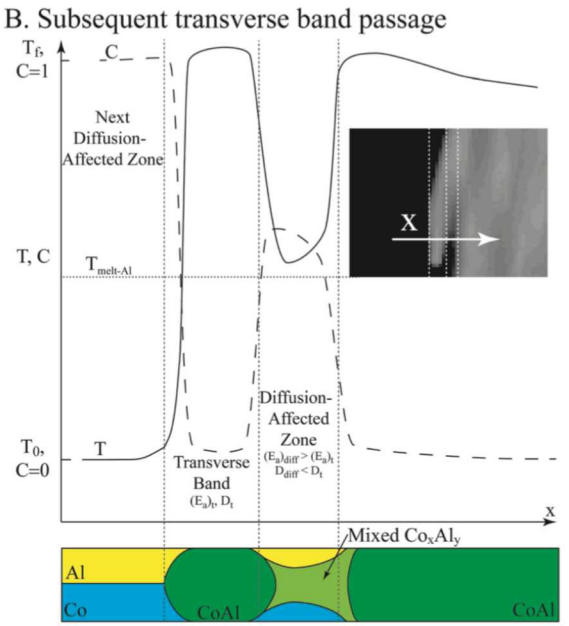

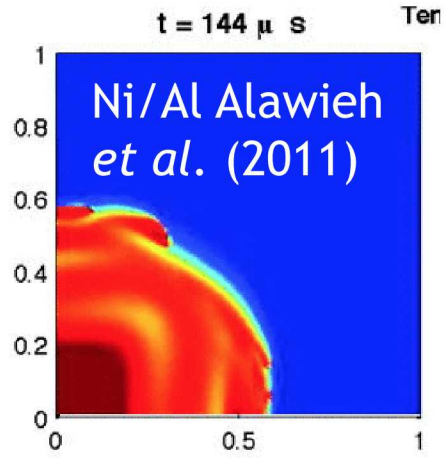

Comparable features have been observed in 3D simulations (qualitative so far)

Objectives

Implement large 3D computer simulations to gain insight into Co/Al reaction instabilities

- Modeling efforts through the early 2000s considered 1D flame propagation only
- Sandia is uniquely positioned with high performance computing (HPC) resources to perform high-fidelity 3D modeling and simulation
- SIERRA computational framework

Develop an empirically-driven reduced order model for Co/Al

- Captures sub-grid product layer growth

Use simulation results to inform a mechanism of instability

- Reeves and Adams (2014) model
- Enthalpy-based stability criteria discussion

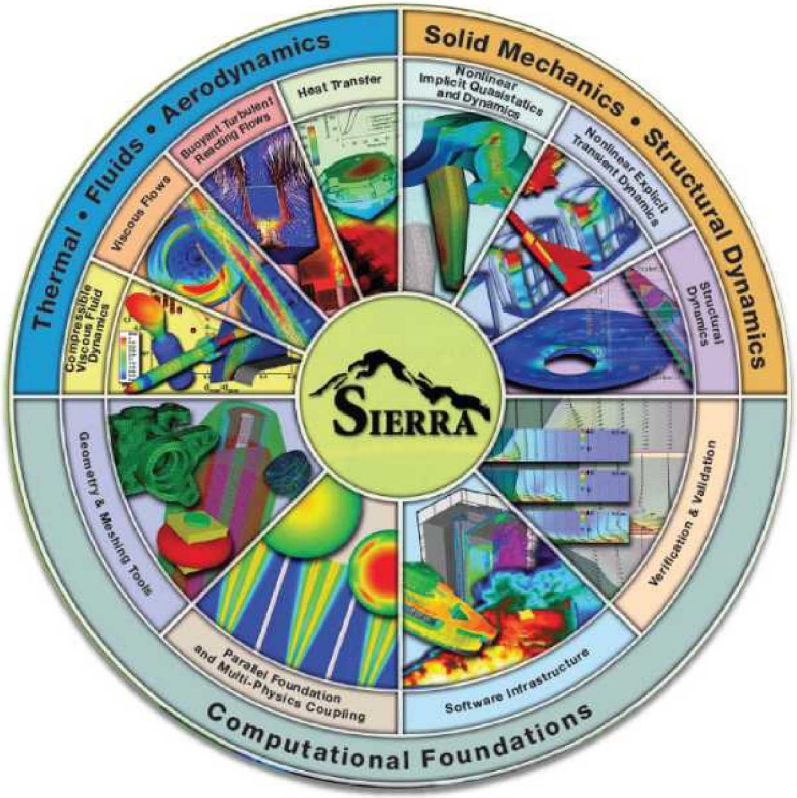

COMPUTATIONAL DETAILS

Simulation Geometry and Computational Limitations

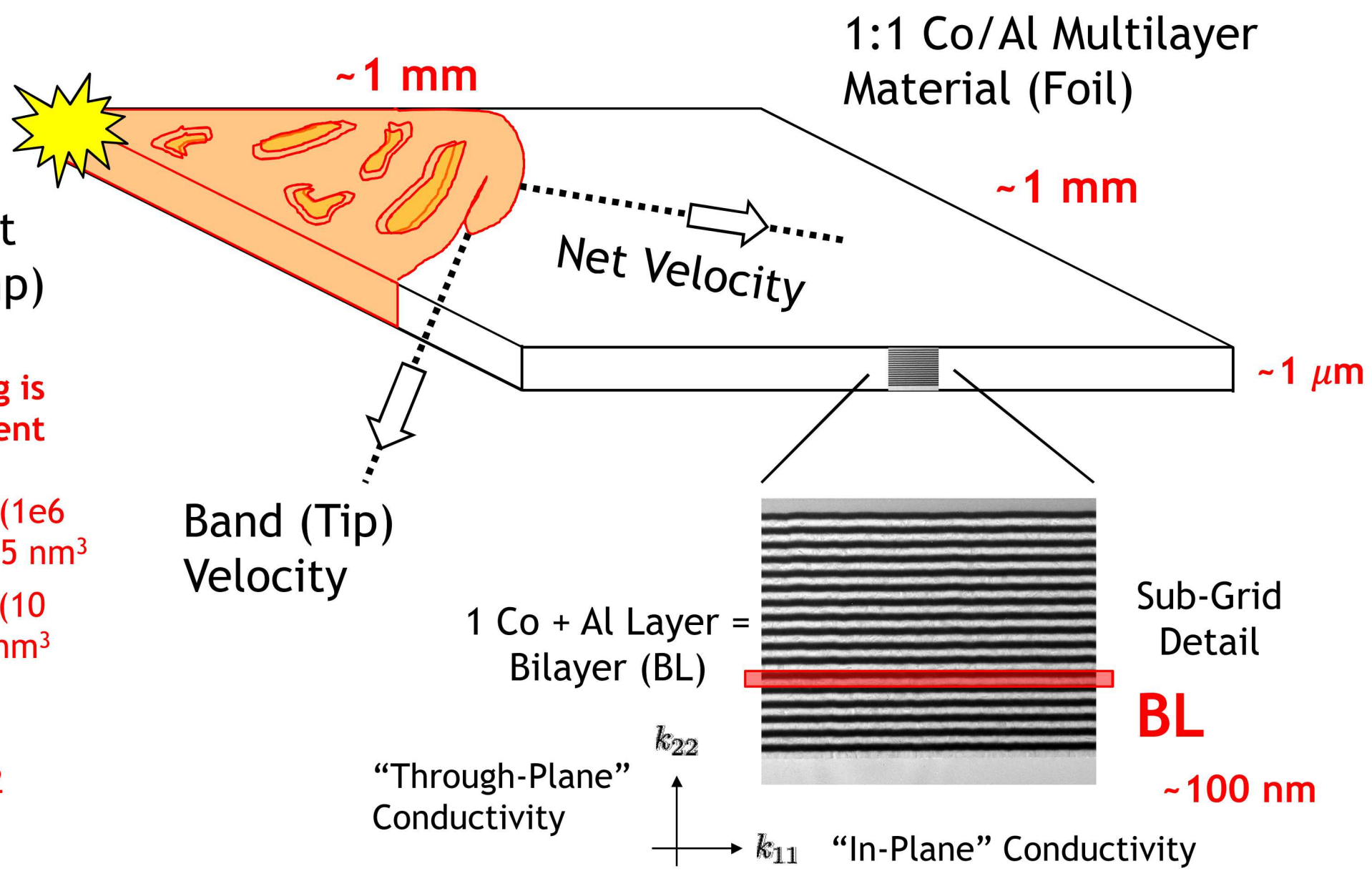

Layer-explicit meshing is not feasible with current HPC resources

- Volume = (1e6 nm)*(1e6 nm)*(1e3 nm) = 1e15 nm^3
- Cell Size = (10 nm)*(10 nm)*(10 nm) = 1e3 nm^3 ~still coarse
- Total Elements = (1e15)/(1e3) = 1e12

1 Trillion Elements!!!

Simulation Geometry – Channel, Corner, and Notched Slab

Thin Channel
~ 10 to 100 K elements

- Uniform hexahedral elements

$$\Delta x = \Delta y = \Delta z = \Delta h$$

- Mesh resolution is either 1 μm or 0.5 μm depending on flame speed (cutoff is ~3 m/s)
- Adaptive time step ~20 ns
- ~50,000 cycles to reach 1 ms

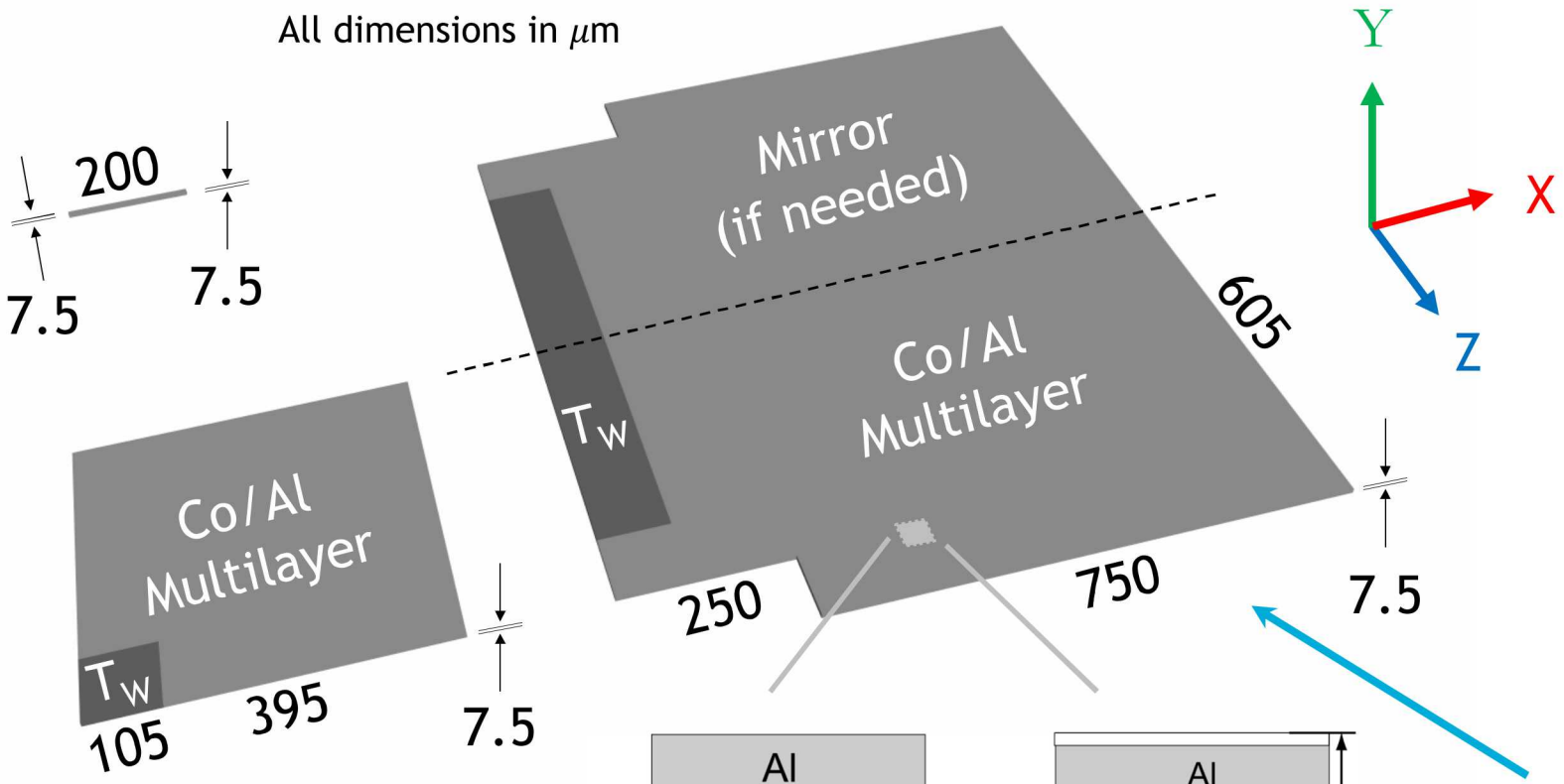

Square Corner ~ 2 M elements

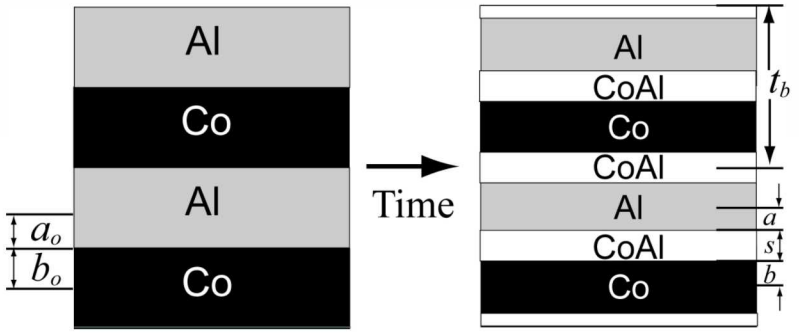

Reduced model is based on Hardt and Phung Diffusion-Limited Reaction Model

Notched Slab
~ 10 M elements

Alternative reduced order models include:

- Besnoin *et al.* (2002)
- Reduced reaction formalism by Salloum and Knio (2010)
- Generalized thermal properties by Alawieh *et al.* (2011)
- 2D phase explicit by Gunduz *et al.* (2009)

Diffusion-Limited Reaction Model by Hardt and Phung (1973)

- Used at SNL by Hobbs *et al.* (2008) to model Co/Al and Al/Pt
- Later extended by Yarrington *et al.* (2017) (2018) and Kittell *et al.* (2018)

$$\rho C_p \frac{\partial T}{\partial t} + \nabla \cdot \boldsymbol{q} = Q\rho \frac{dF}{dt}$$

Atom Diffusivity w/ Arrhenius-Type Diffusion Coefficients(s)
- Product layer growth rate ~ 1/product layer thickness
- Hardt and Phung system of ODEs
- Mass diffusion is piecewise continuous for solid-solid, solid-liquid, liquid-liquid

Heat of Reaction from Calorimetry
- Net heat release from calorimetry data
- Depends on the BL thickness
- Kittell Q-factor for nonlinear species profiles

Thermal Conductivity
- Anisotropic conductivity
- Network of resistors in series (in-plane) or parallel (through-plane)
- Different values for Co, Al, premix, and product
- Anisotropic drives to isotropic with reaction

Specific Heat
- Mass-weighted heat capacity
- Temperature and phase dependent
- Includes latent enthalpies via mush zone
- Irreversible phase change

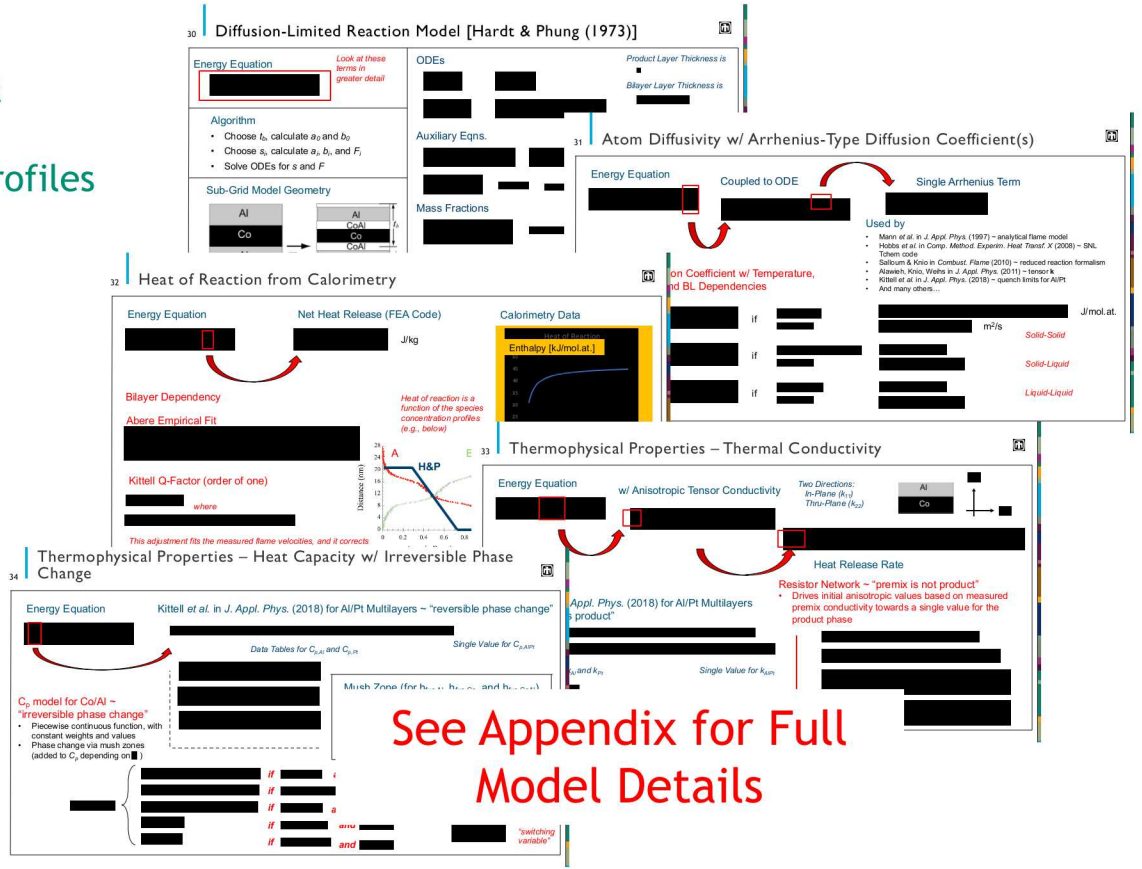

See Appendix for Full Model Details

RESULTS

Trends in BL Thickness – Net and Band Propagation Velocity

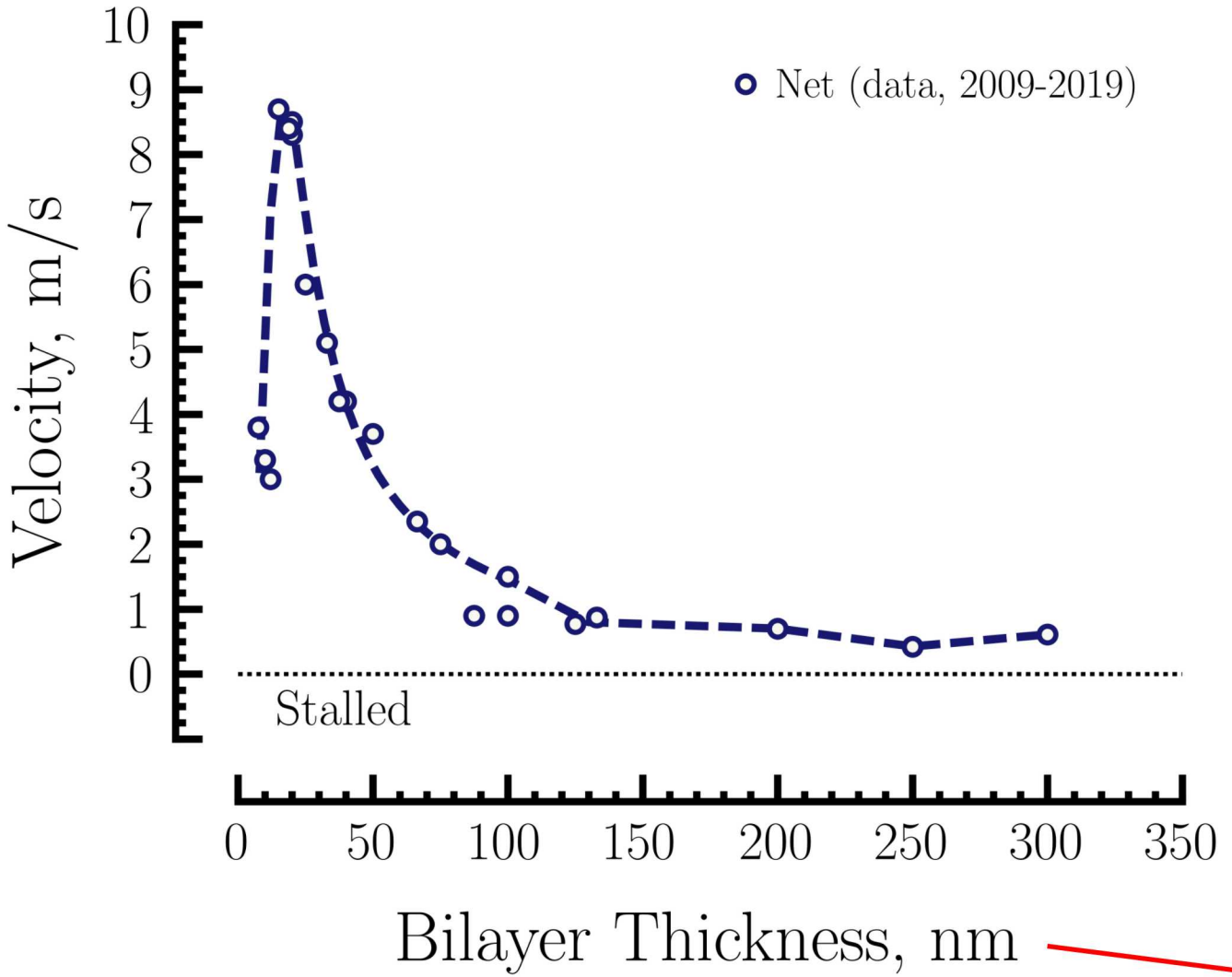

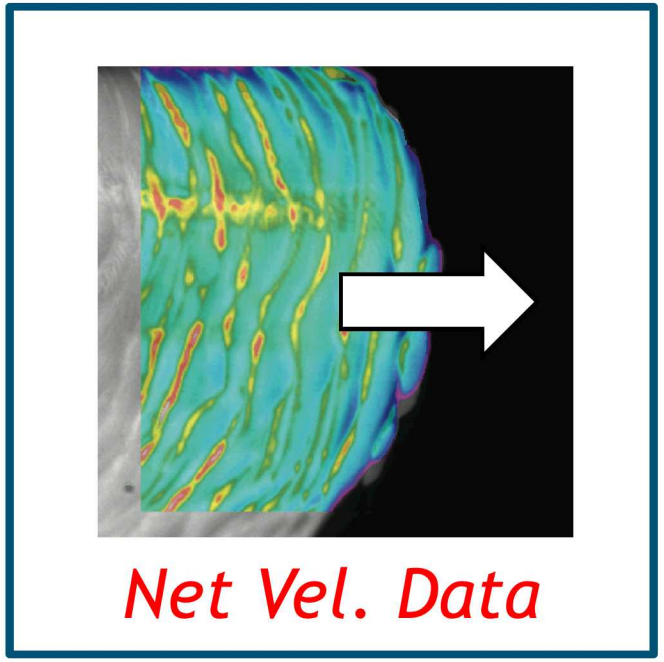

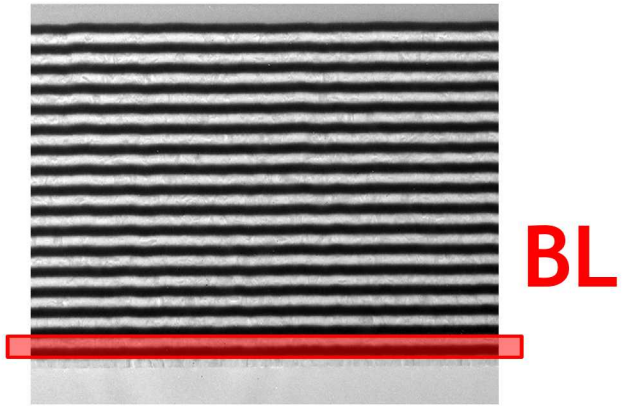

Trends in BL Thickness – Net and Band Propagation Velocity

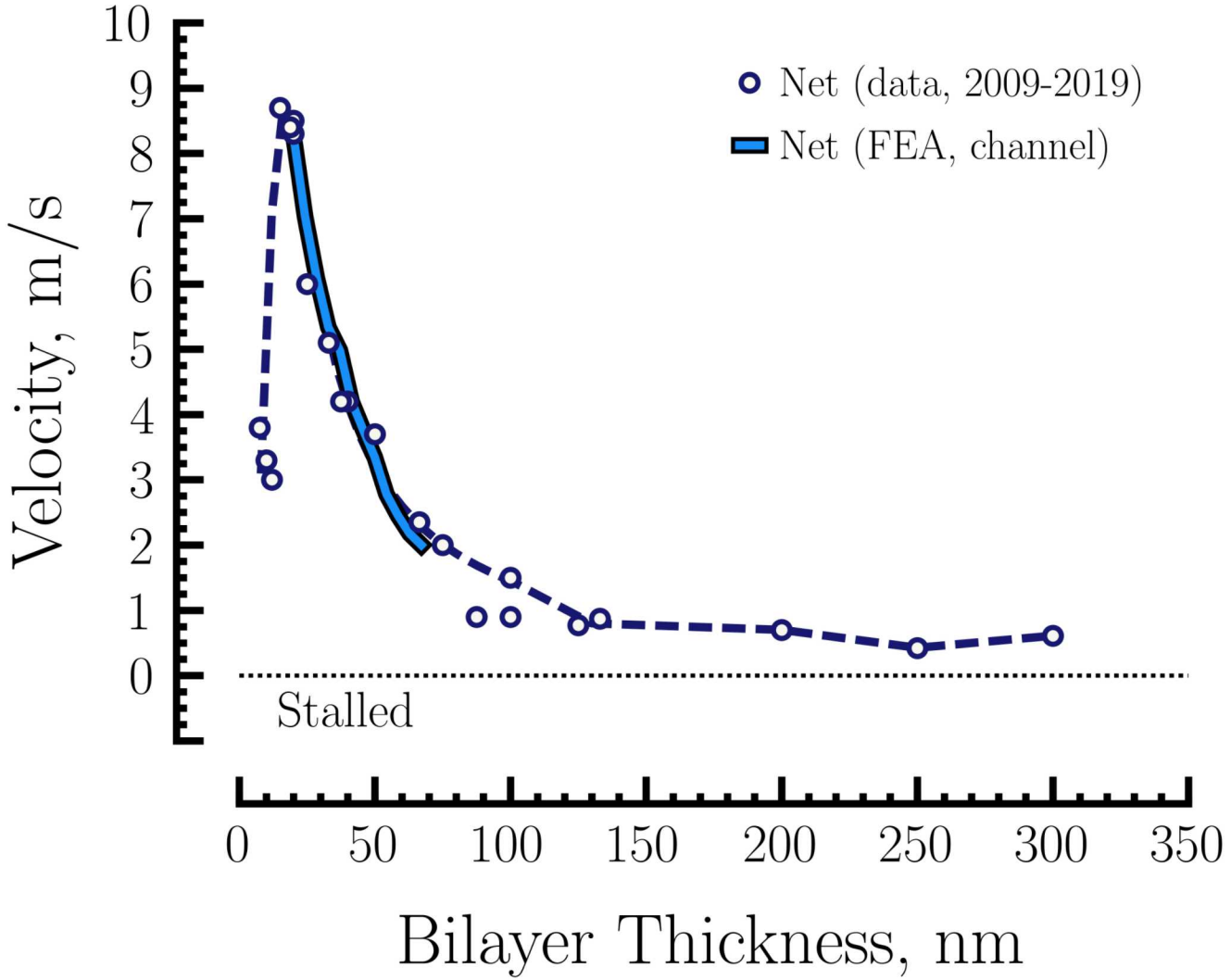

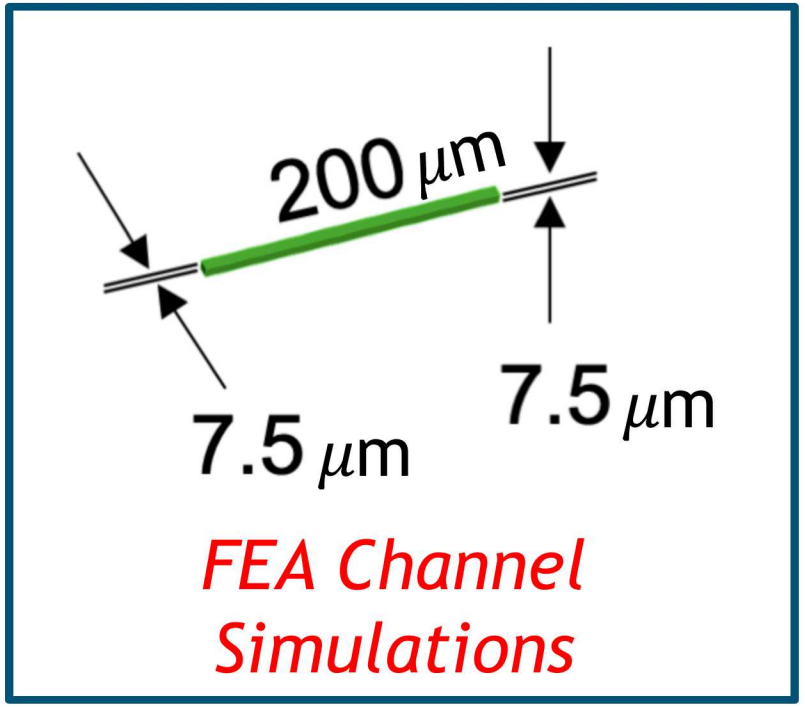

Trends in BL Thickness – Net and Band Propagation Velocity

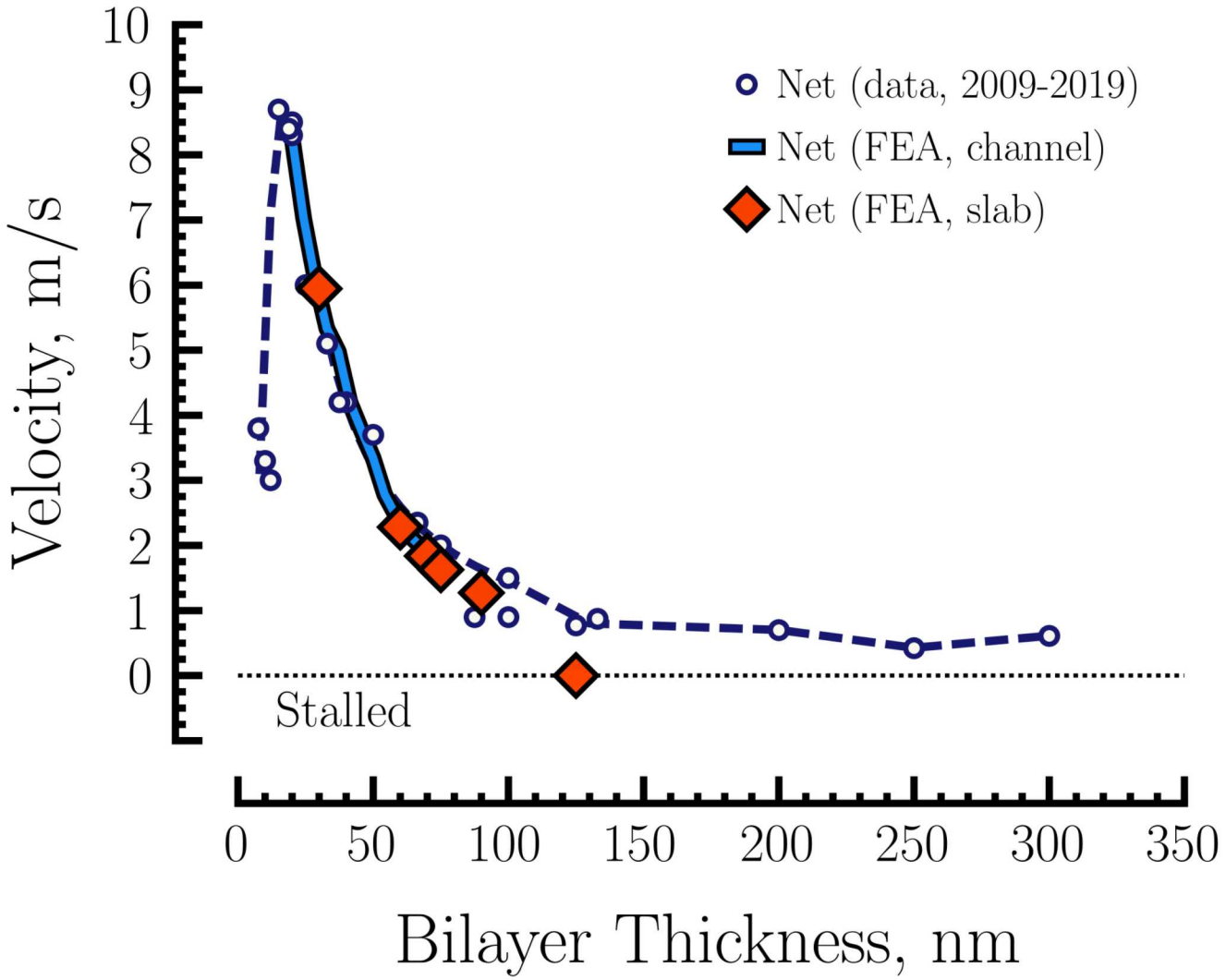

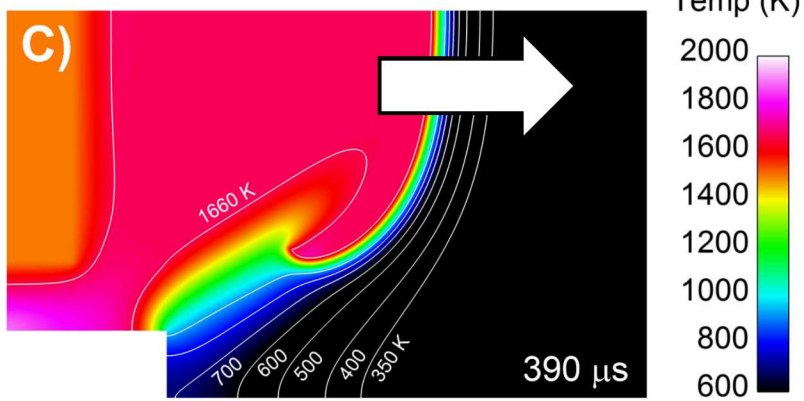

FEA Notched Slab Simulations

Trends in BL Thickness – Net and Band Propagation Velocity

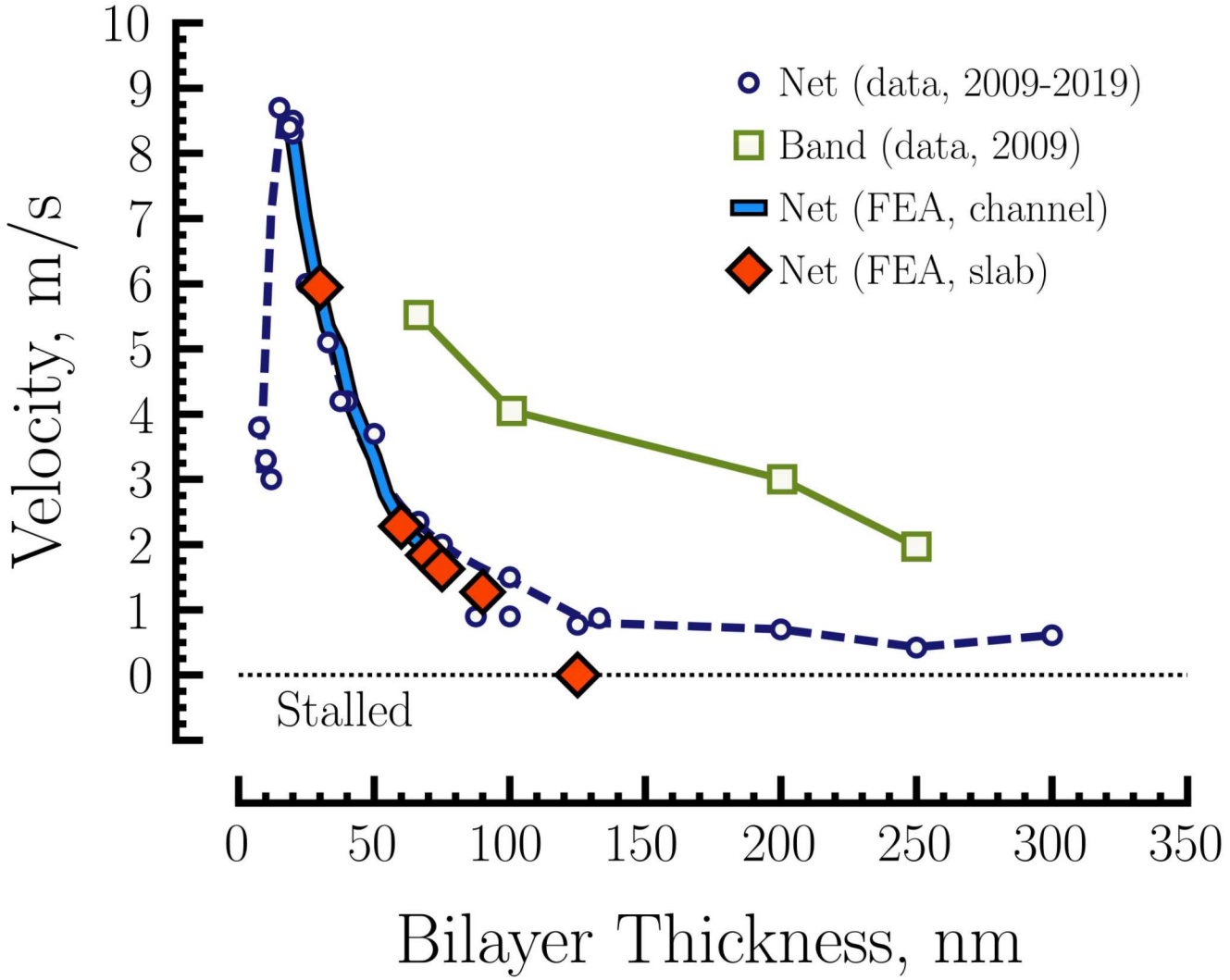

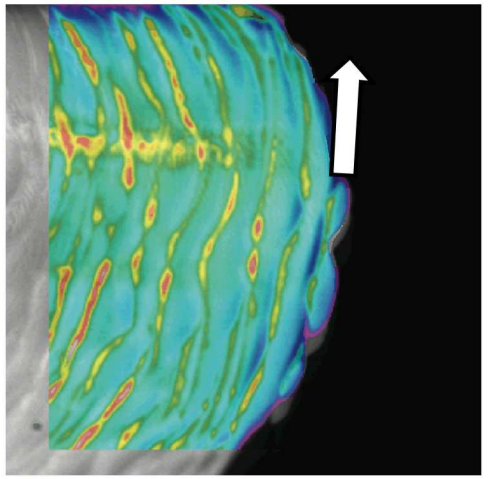

Band Vel. Data

Trends in BL Thickness – Net and Band Propagation Velocity

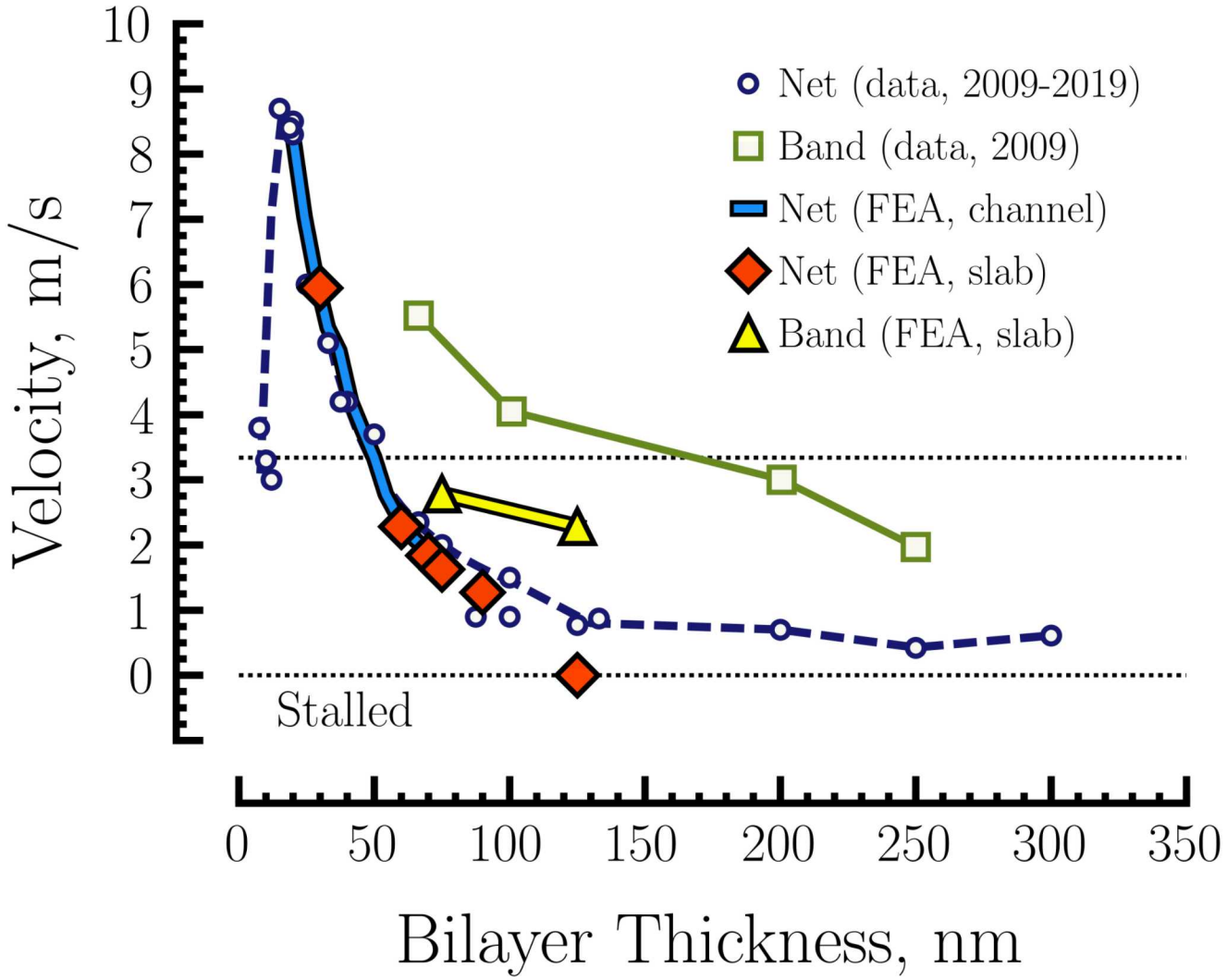

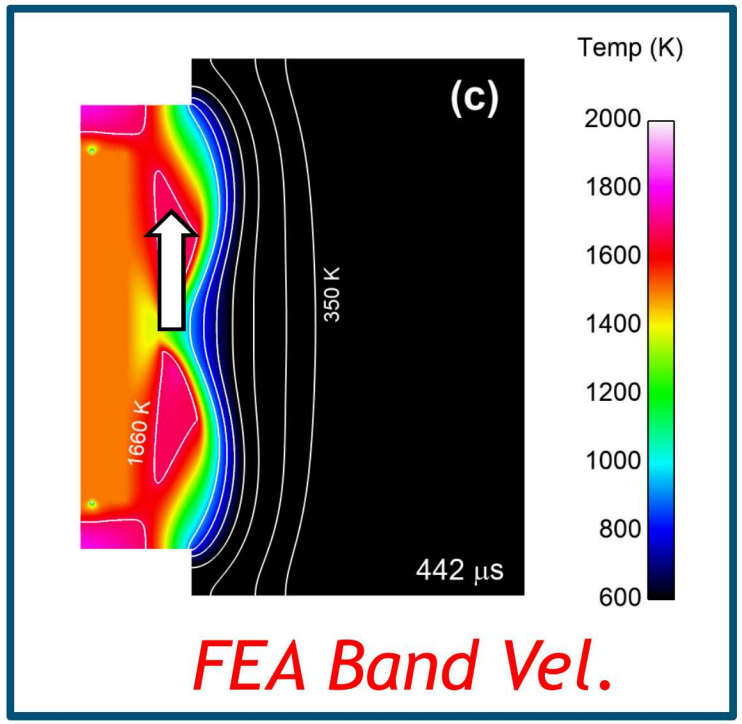

Trends in BL Thickness – Net and Band Propagation Velocity

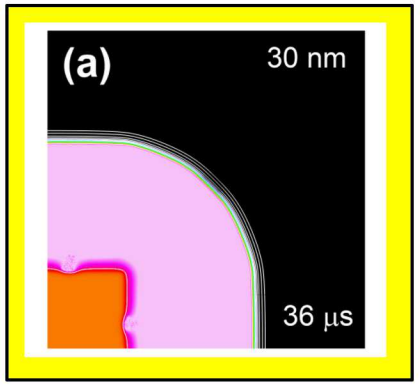

30 nm

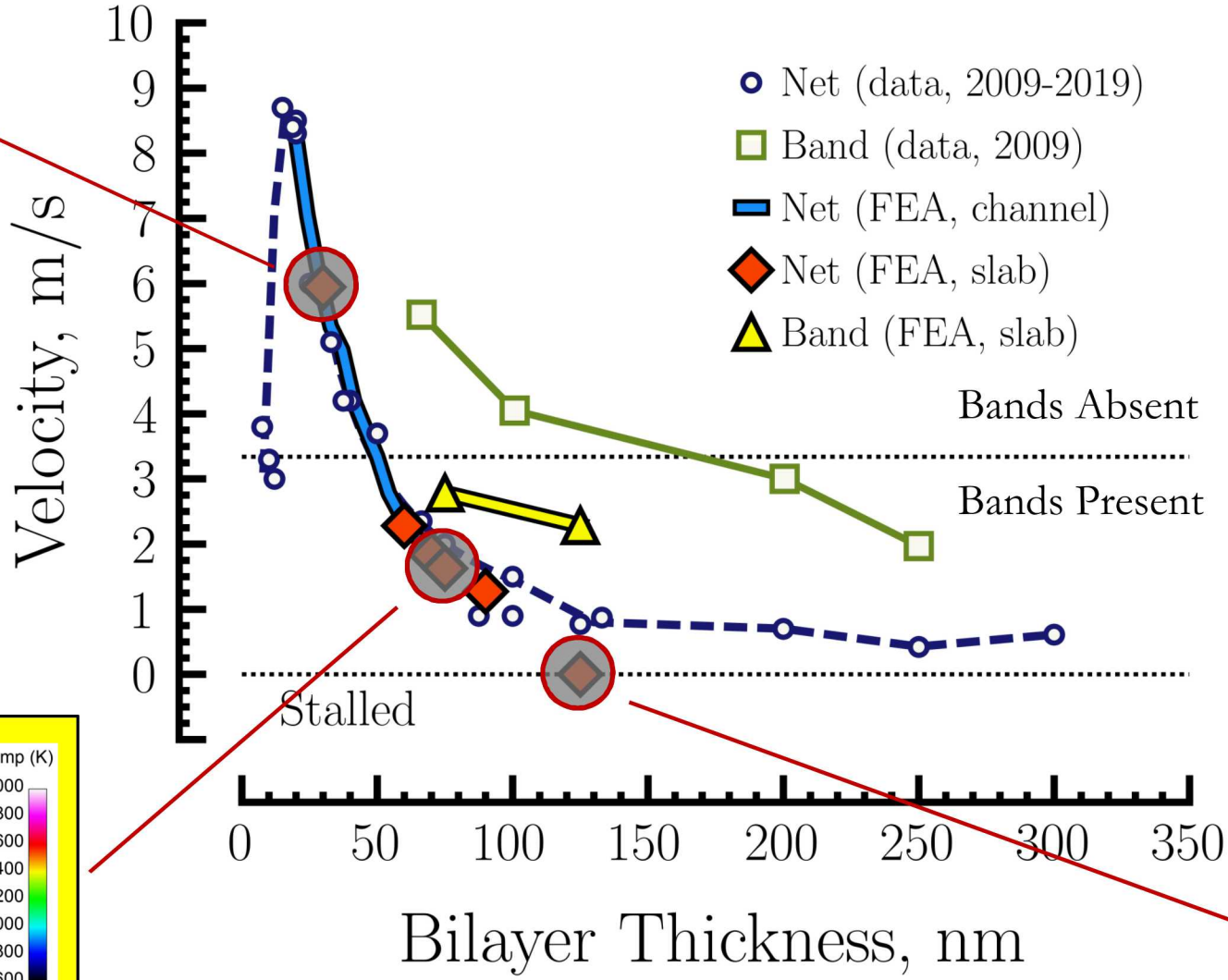

75 nm

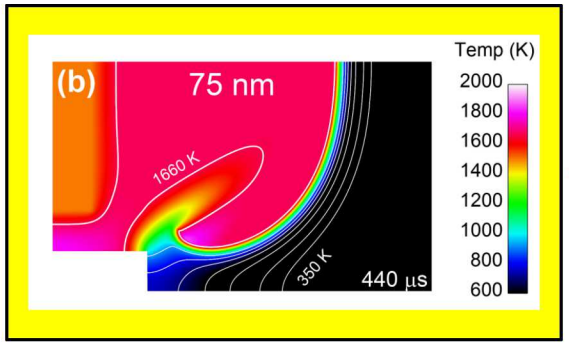

- All data for total film thickness 7.5 μm
- Reeves and Adams (2014) were the first to observe a correlation between stability and a velocity limit ~3 m/s

125 nm

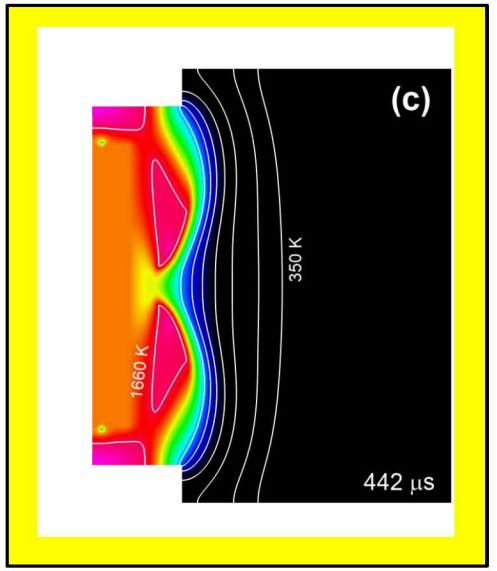

Trends in BL Thickness – Flame Temperature from Simulations

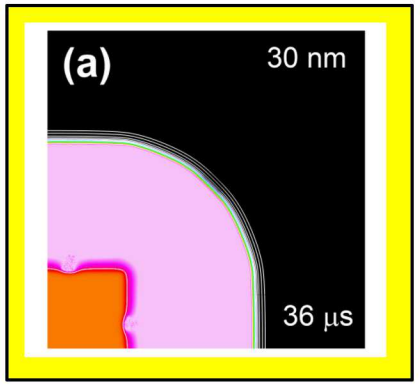

30 nm

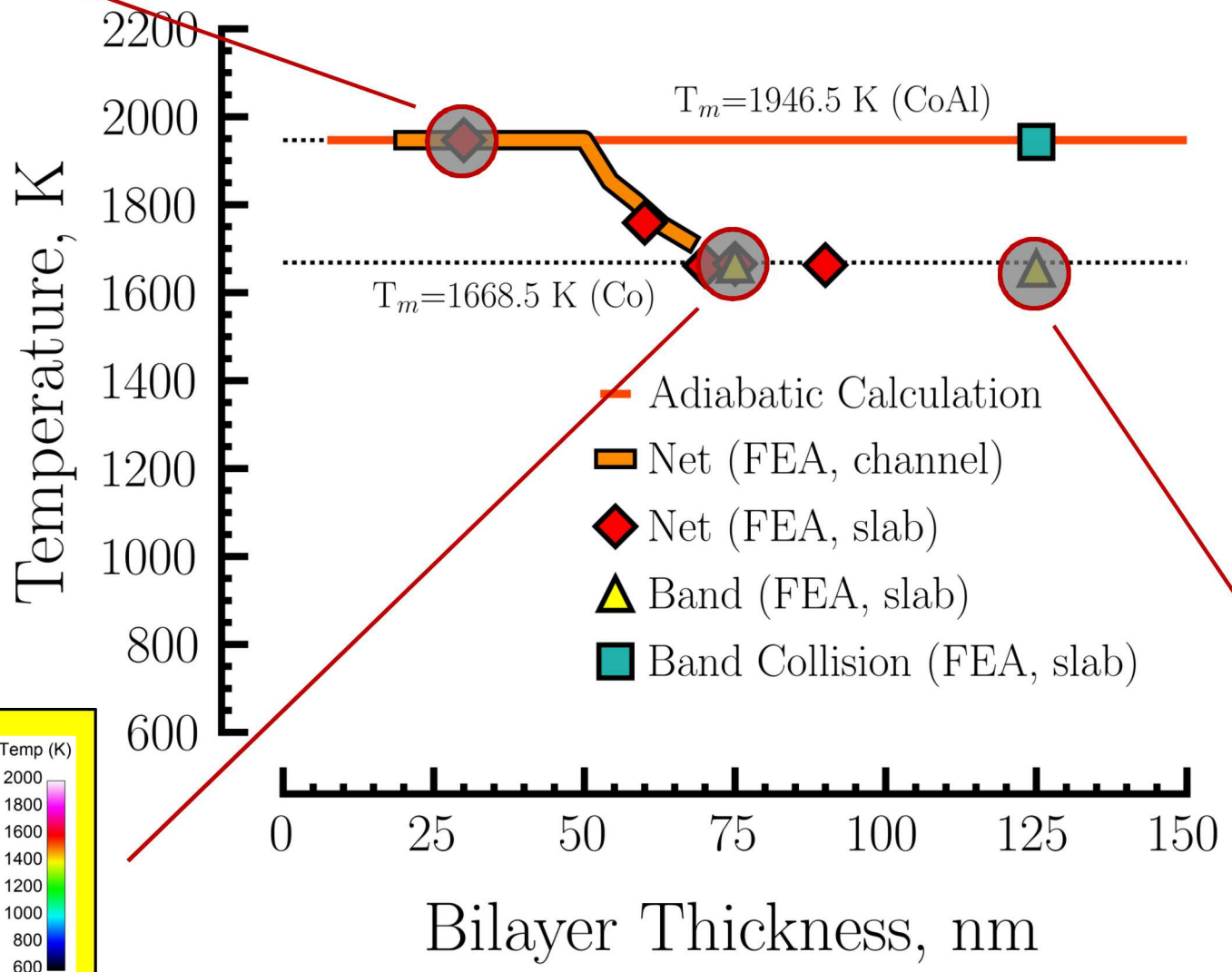

- Adiabatic flame temperature from enthalpy-temperature diagram, see later slide
- Deviation from adiabatic flame temp occurs ~50 nm
- Net and band flame temperatures tend to ride along the melt isotherms

75 nm

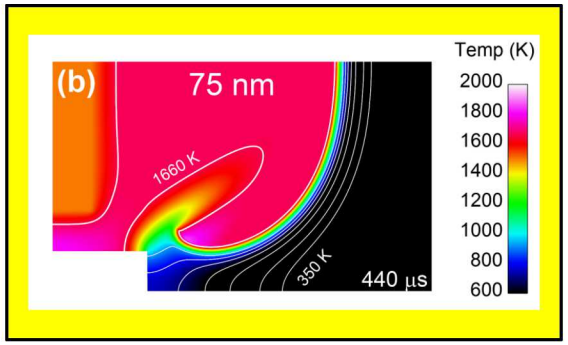

125 nm

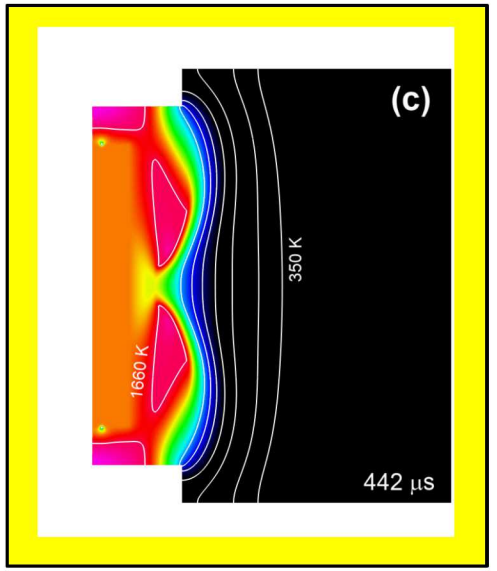

Trends in BL Thickness – Temperature Gradient from Simulations

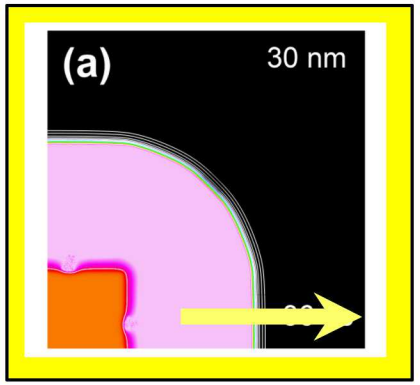

30 nm

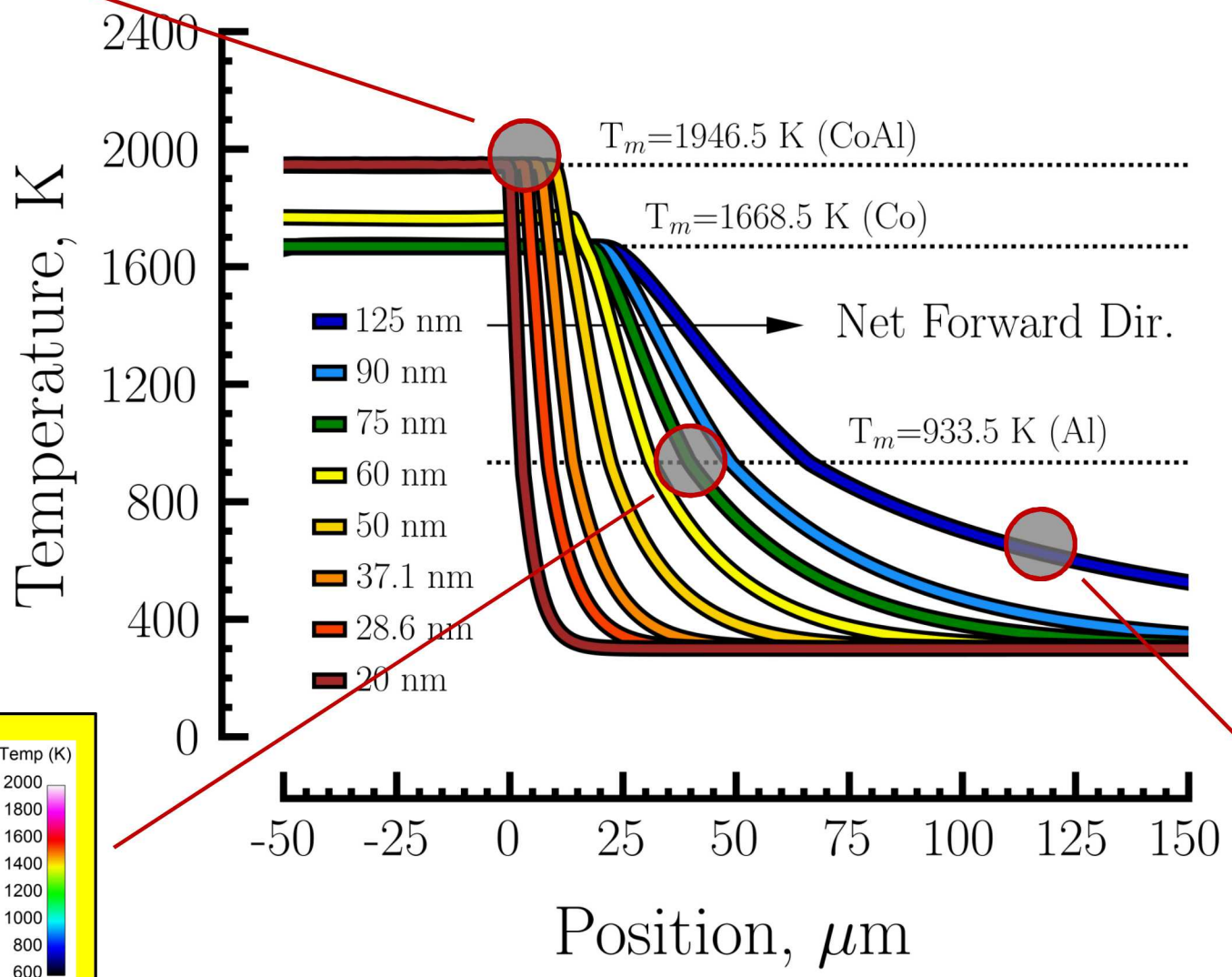

75 nm

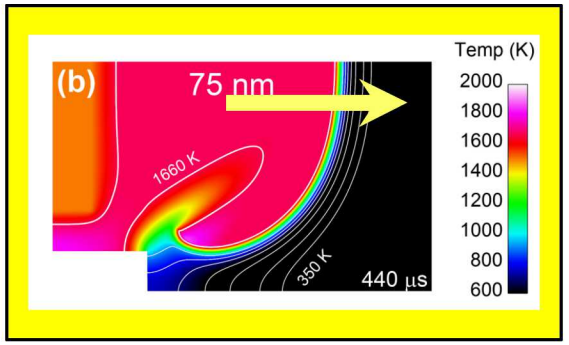

125 nm

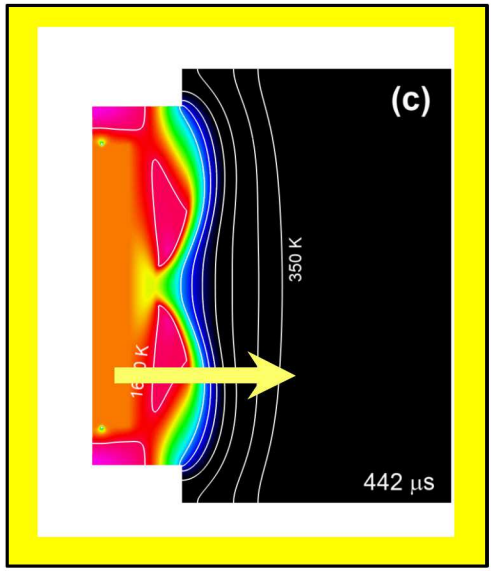

- Forward conduction loss varies with BL thickness
- Similar to having a multilayer on a substrate (see Kittell *et al.* (2018) for analysis with quench limits)

30 nm BL Thickness / Steady Propagation

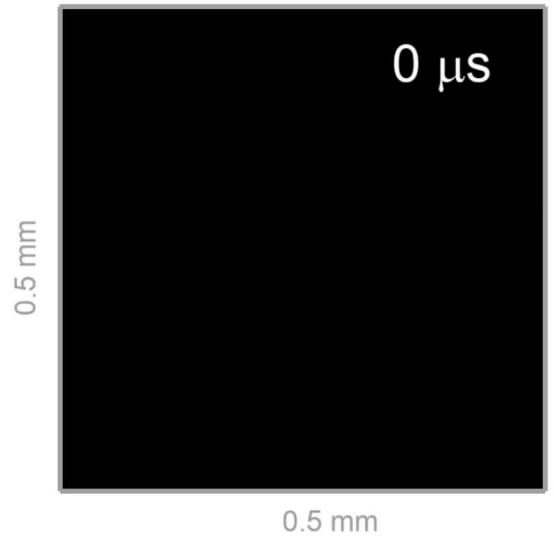

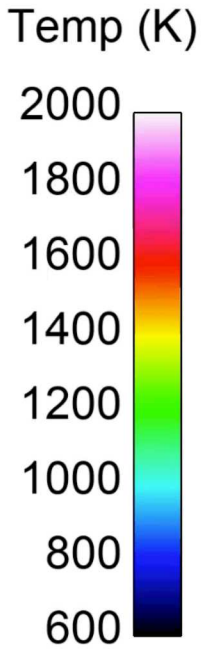

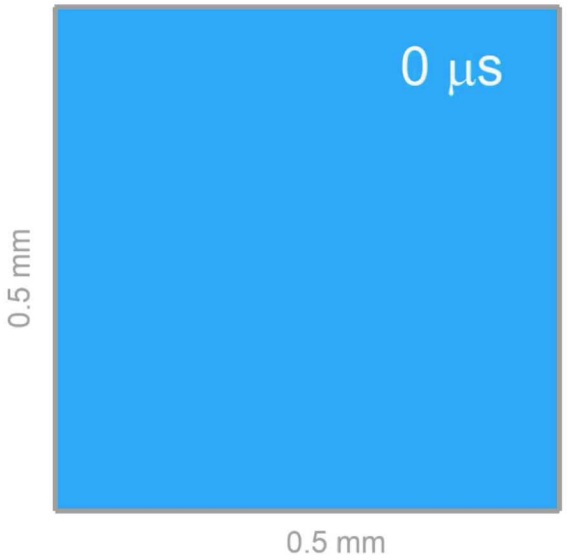

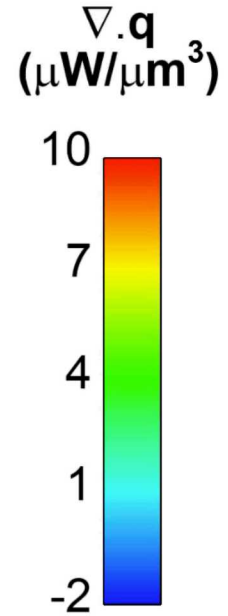

- Steady velocity and temperatures match FEA channel geometry simulation
- Sharp symmetry and stiff chemistry make eliminating numerical errors very hard
- Numerical errors can trip physical mechanisms for instability, but not the case here w/ 30 nm BL, Co/Al

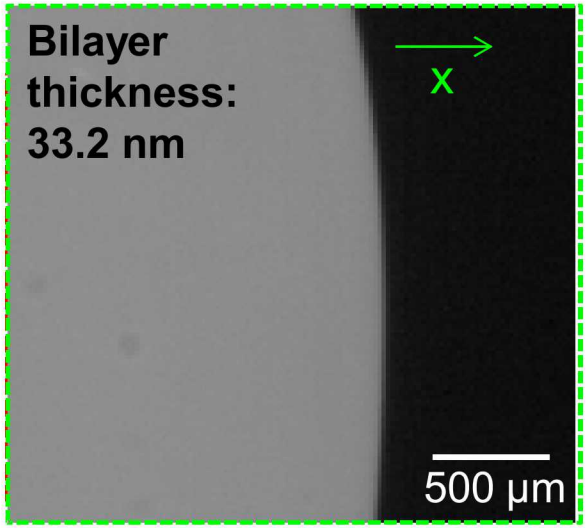

Real Wavefront Morphology

75 nm BL Thickness / Mode I Instability

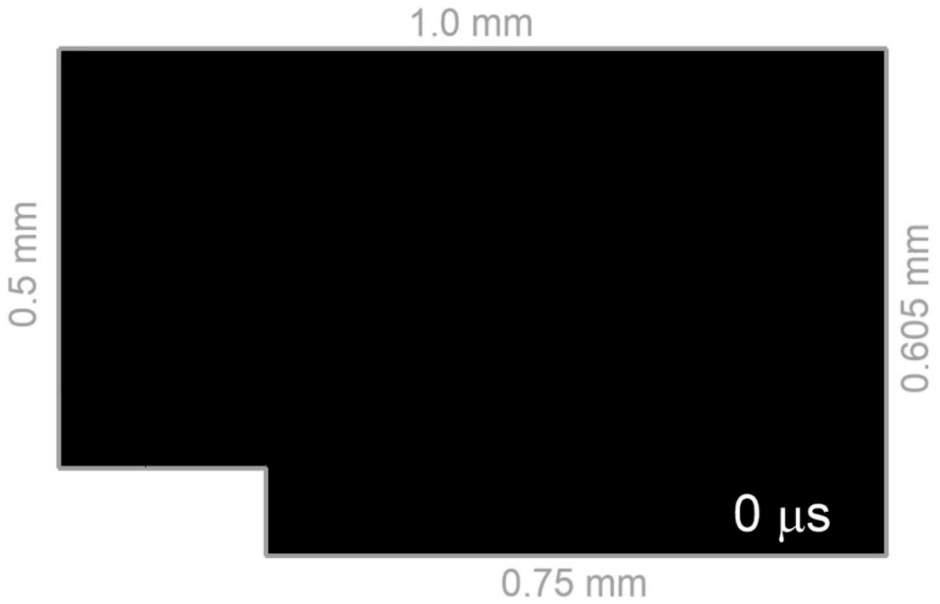

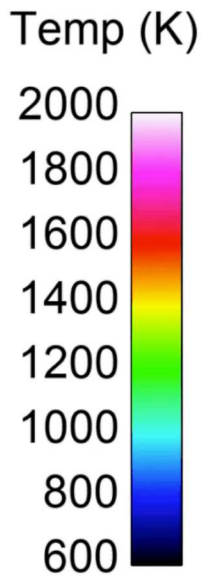

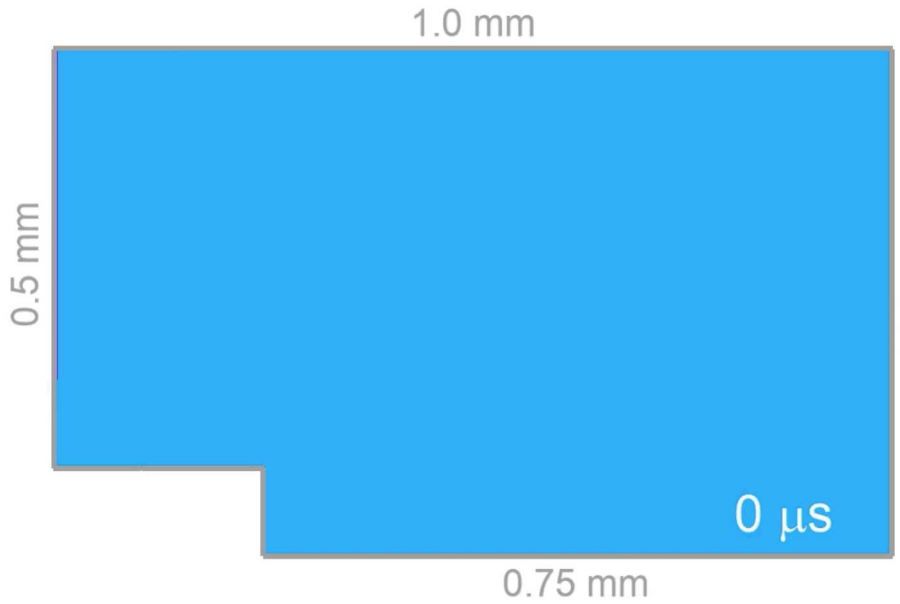

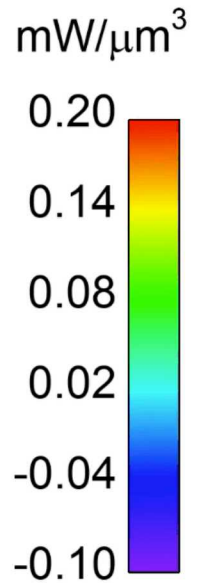

- ❑ Front self-propagates, but may "shed" spin bands from the edges
- ❑ High-Explosives (HE) analogue: detonation corner turning

Image From:
Schwendeman, Kapila, and Henshaw (2010)

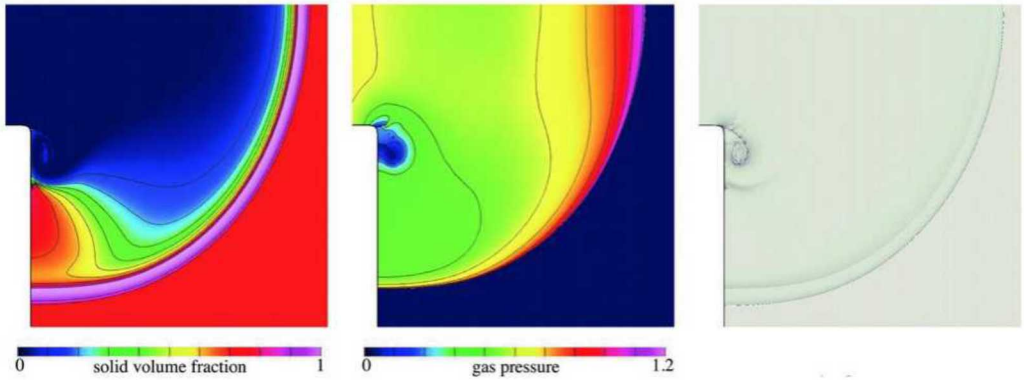

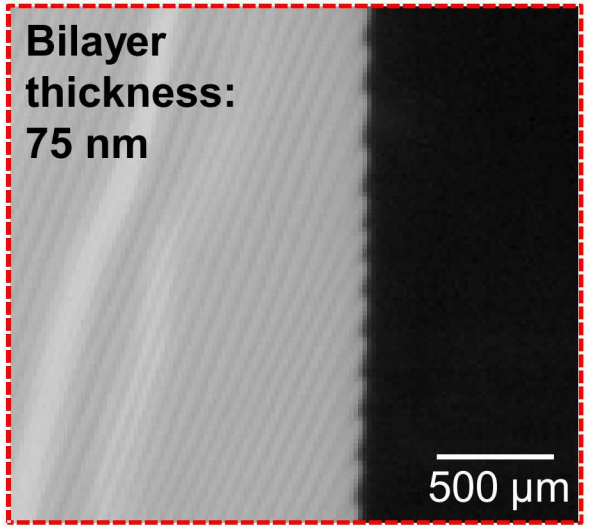

Real Wavefront Morphology

125 nm BL Thickness / Mode II Instability

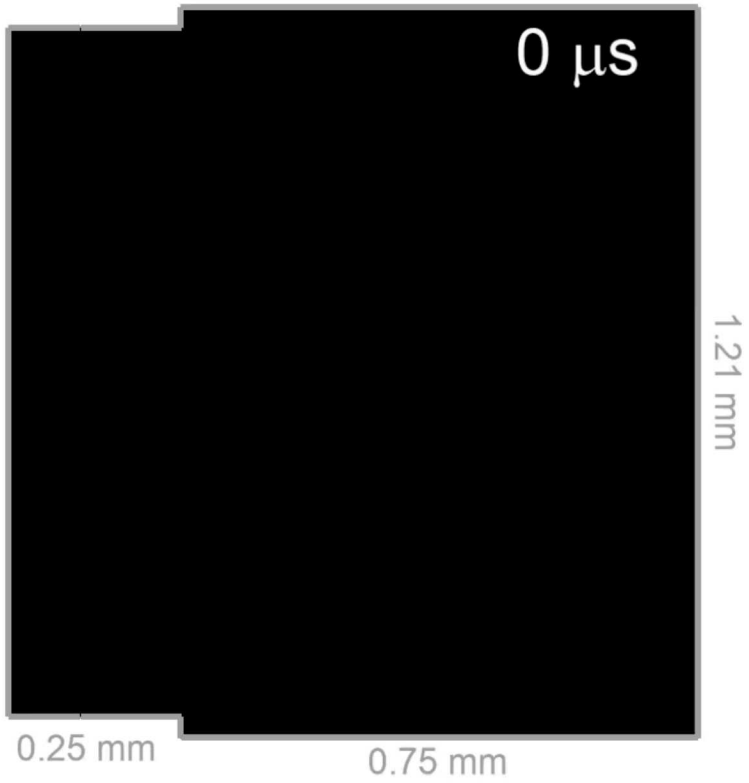

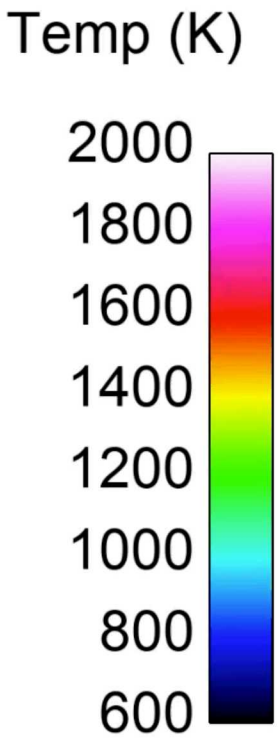

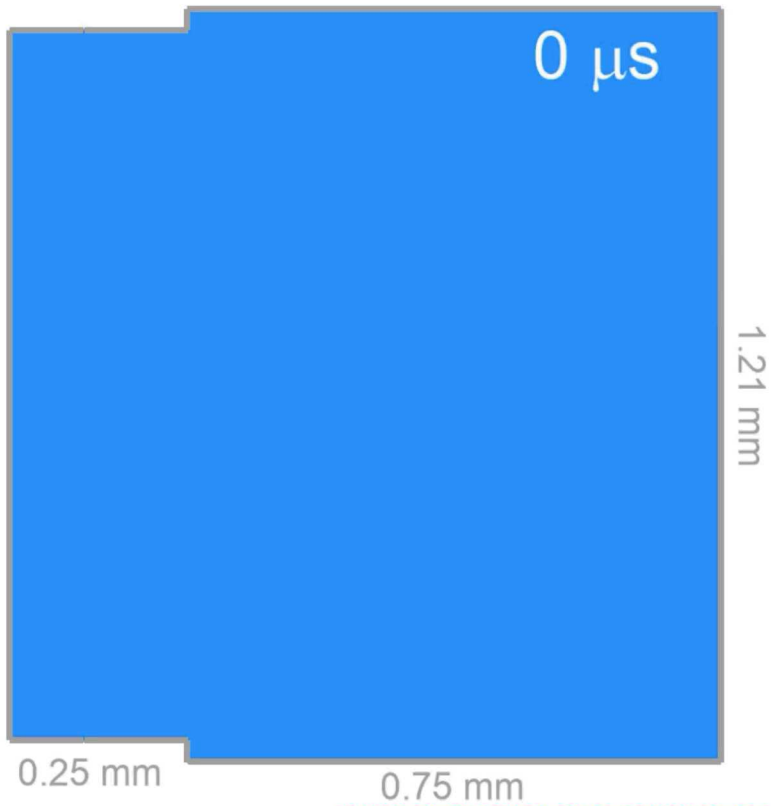

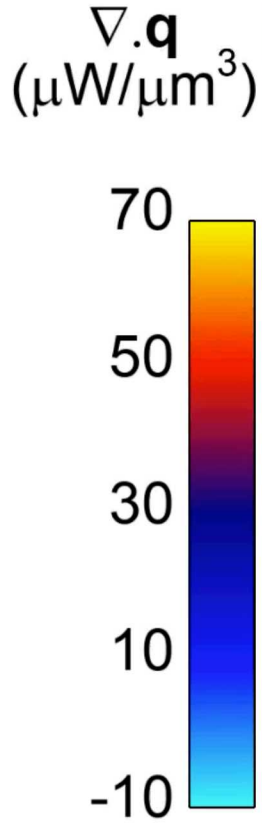

- Stalled front in normal direction
- Spin band collision moves front forward

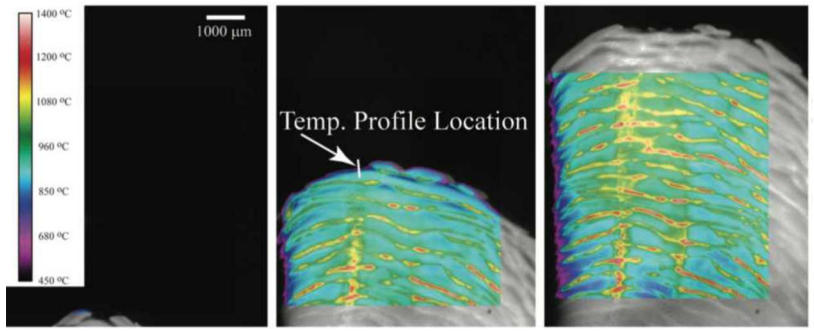

Image From: Reeves and Adams (2014)

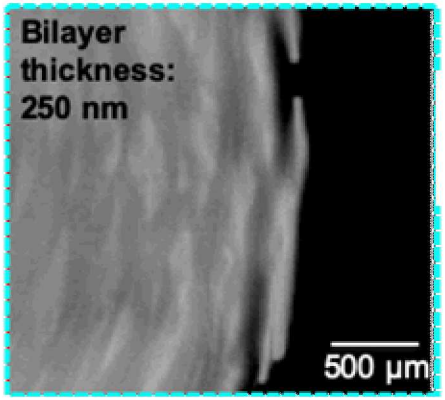

Real Wavefront Morphology

75 nm BL Thickness / Mode I: Spin Band Interrogation

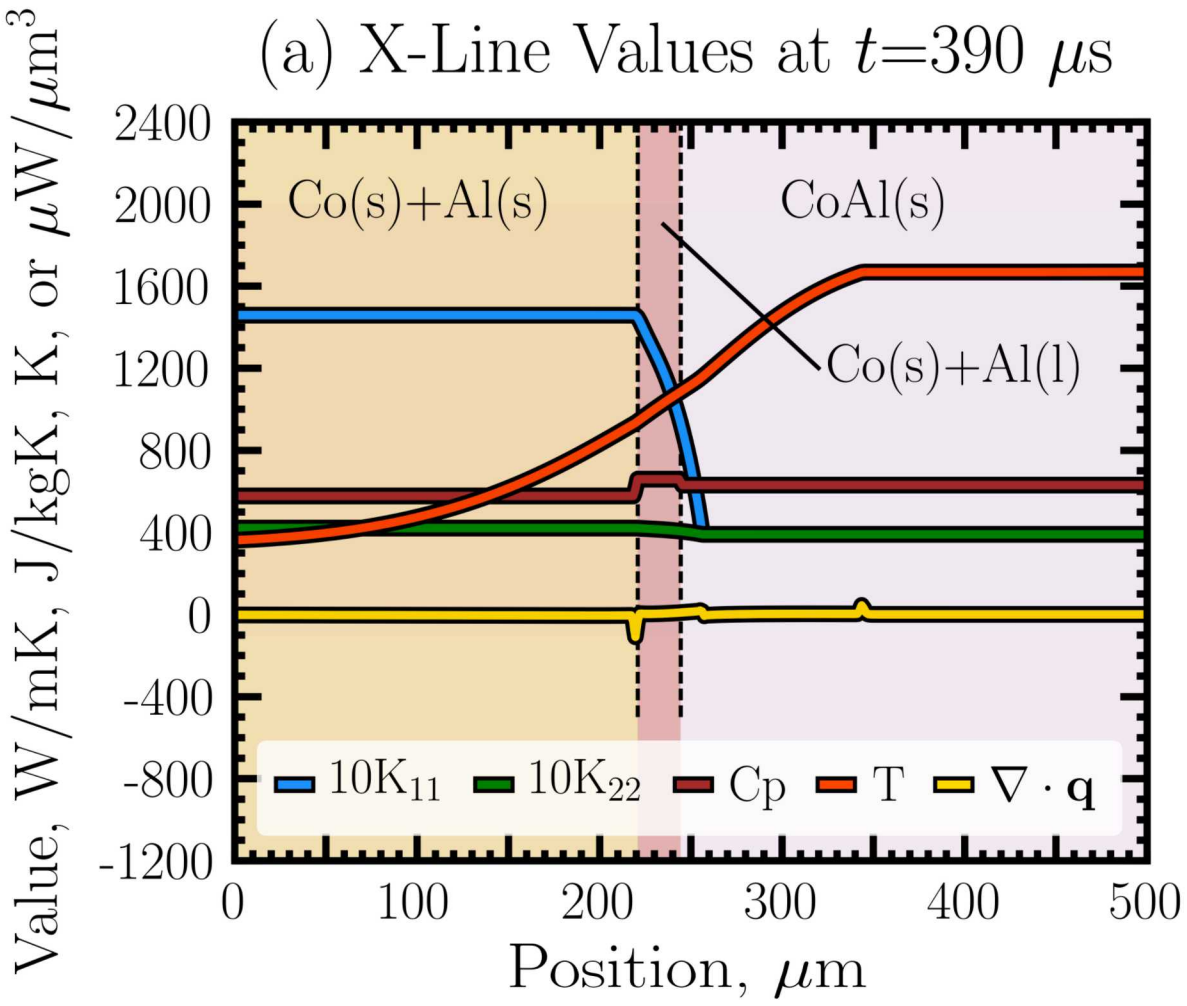

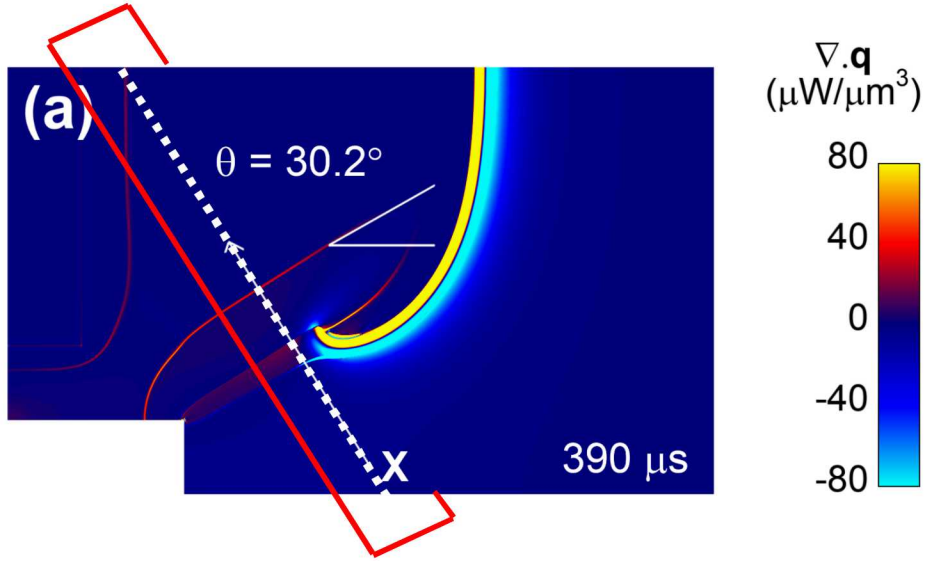

X-Line is *BEFORE* the spin band

- Thermal conduction losses ahead of the front are too high for a self-propagating flame
- Thermally-affected area is greater than the Chemically-affected region (w/ phase change)
- Tensor k_{11} and k_{22} are a function of product layer thickness alone (i.e. Blue curve shows the reaction zone thickness)

75 nm BL Thickness / Mode I: Spin Band Interrogation

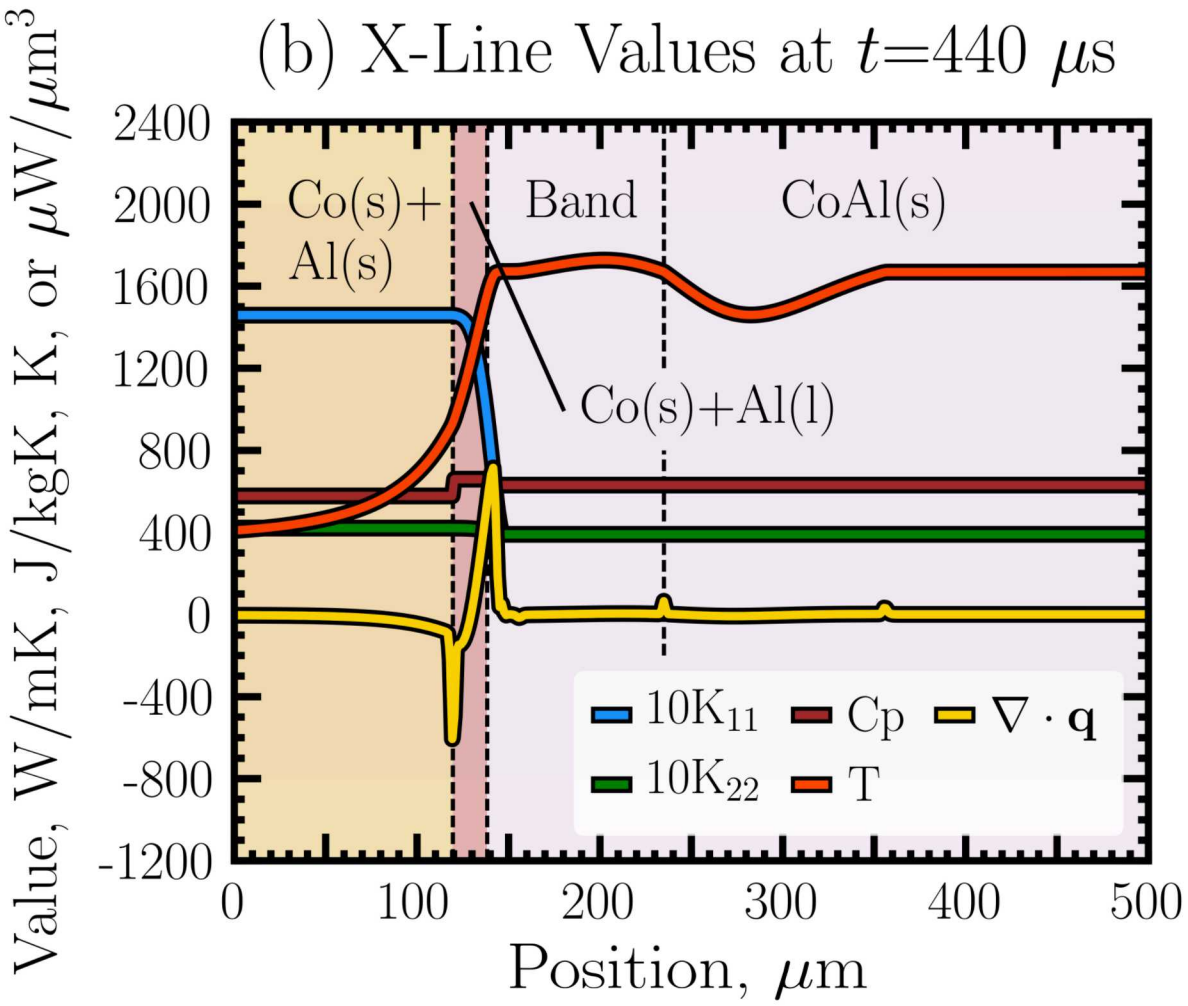

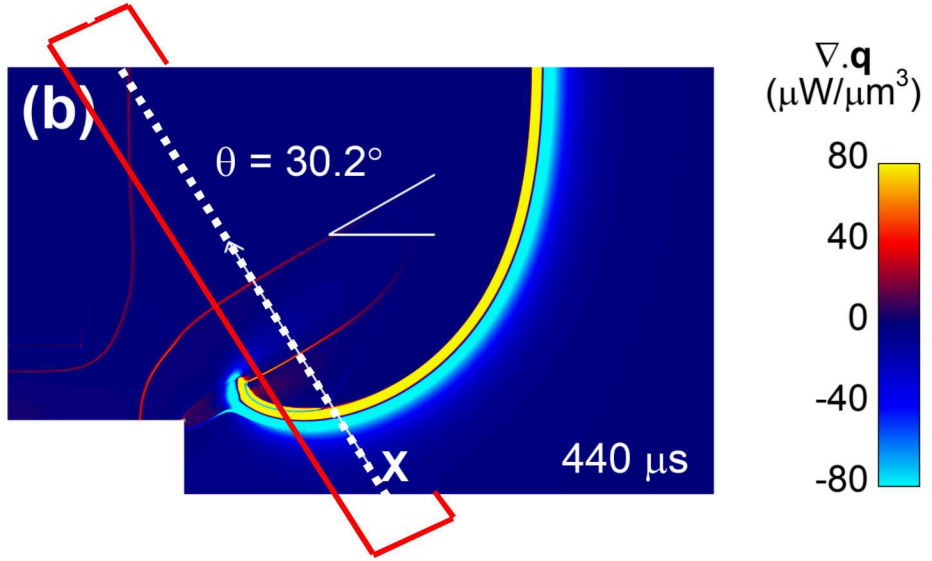

X-Line is *THROUGH* the spin band

- Thermal conduction losses are now lower
- Propagates in the direction of the band tip, as well as in the outward bulk direction
- Thermal deficit behind the font; could this be used to define a band thickness?
- Residual Co in mixture model leads to solidification exotherms (faint red lines)

75 nm BL Thickness / Mode I: Spin Band Interrogation

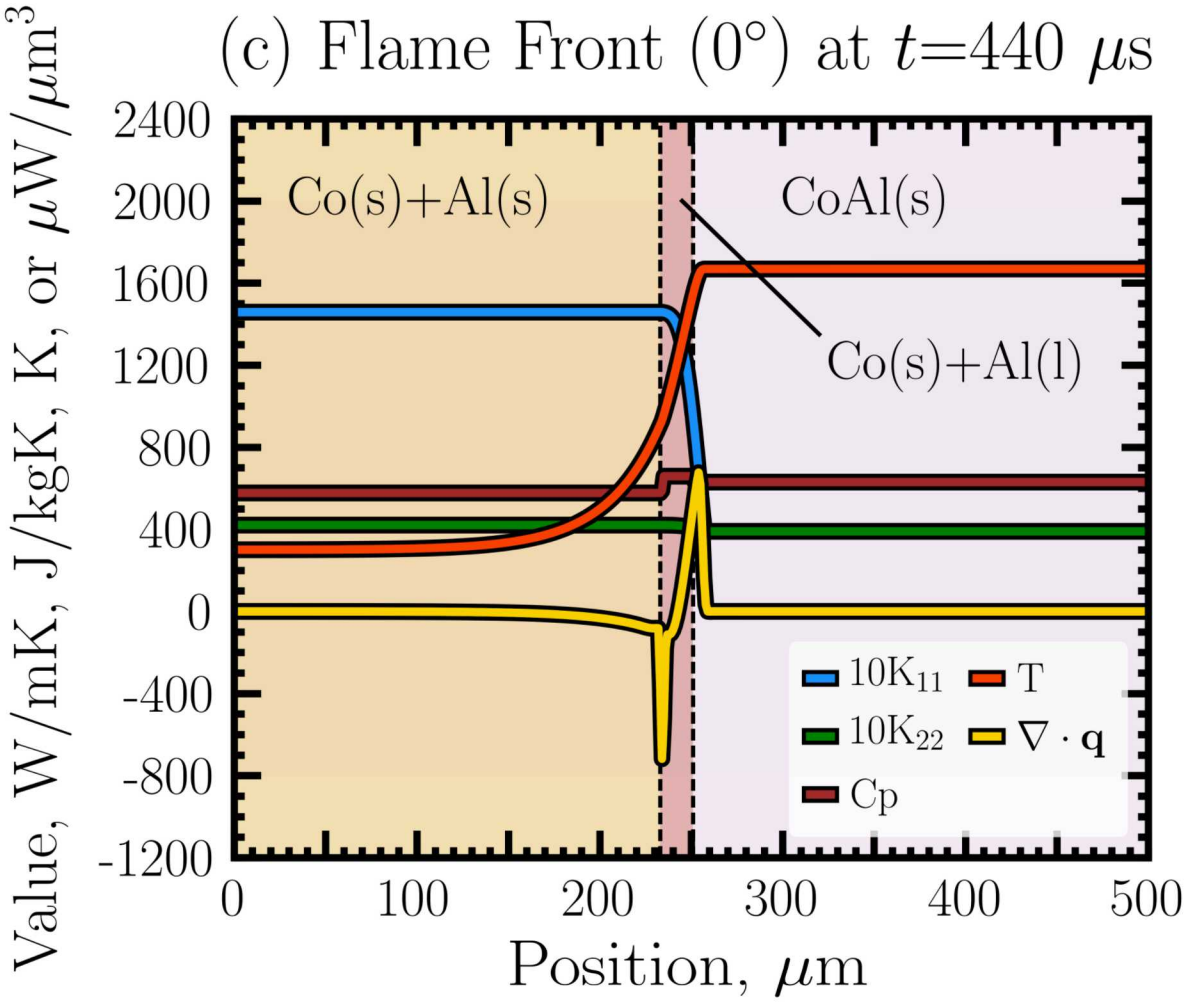

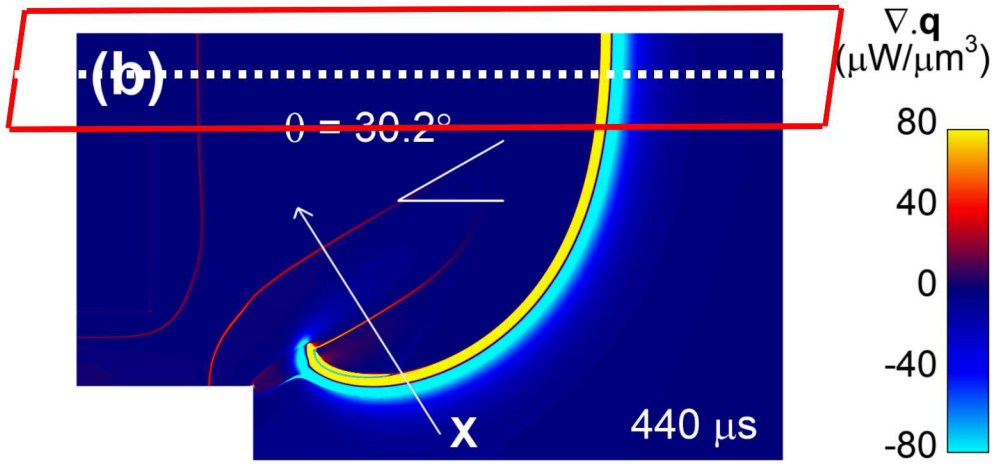

Plot is *THROUGH* the *FLAME FRONT*

- Steady wave propagation along the top edge (minimum z-value)
- Flame temperature is constant at the Co melt
- Flame composition ends in solid product

125 nm BL Thickness / Mode II: Spin Band Interrogation

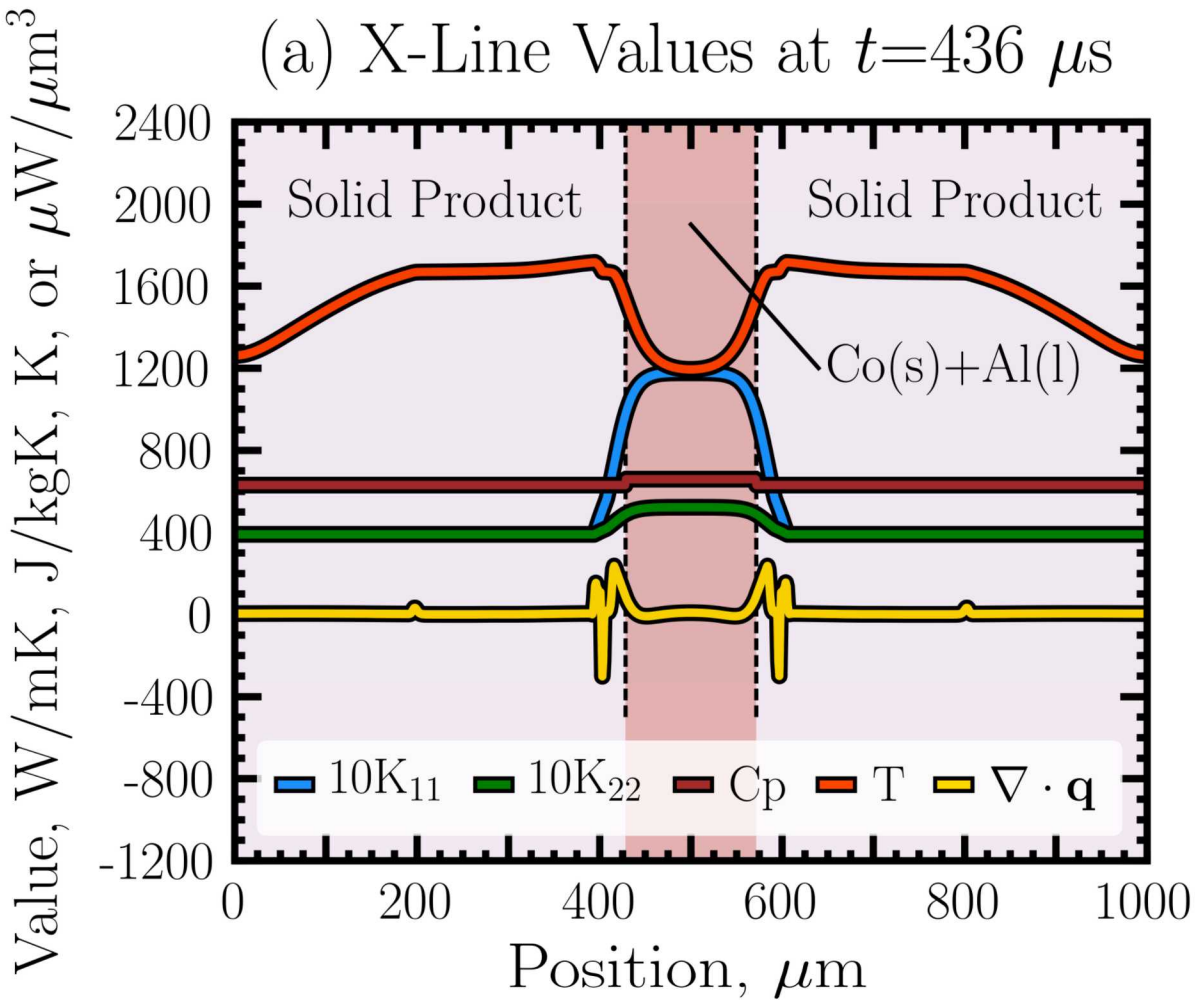

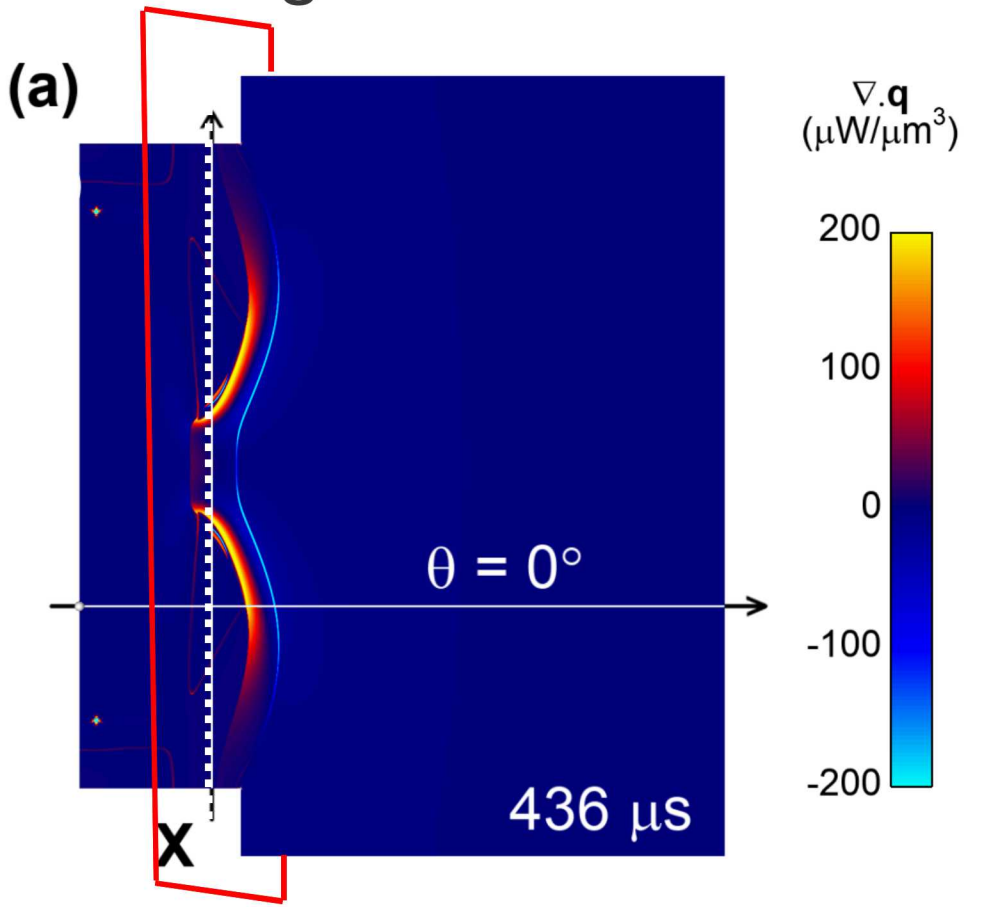

X-Line values are *BEFORE* the collision

125 nm BL Thickness / Mode II: Spin Band Interrogation

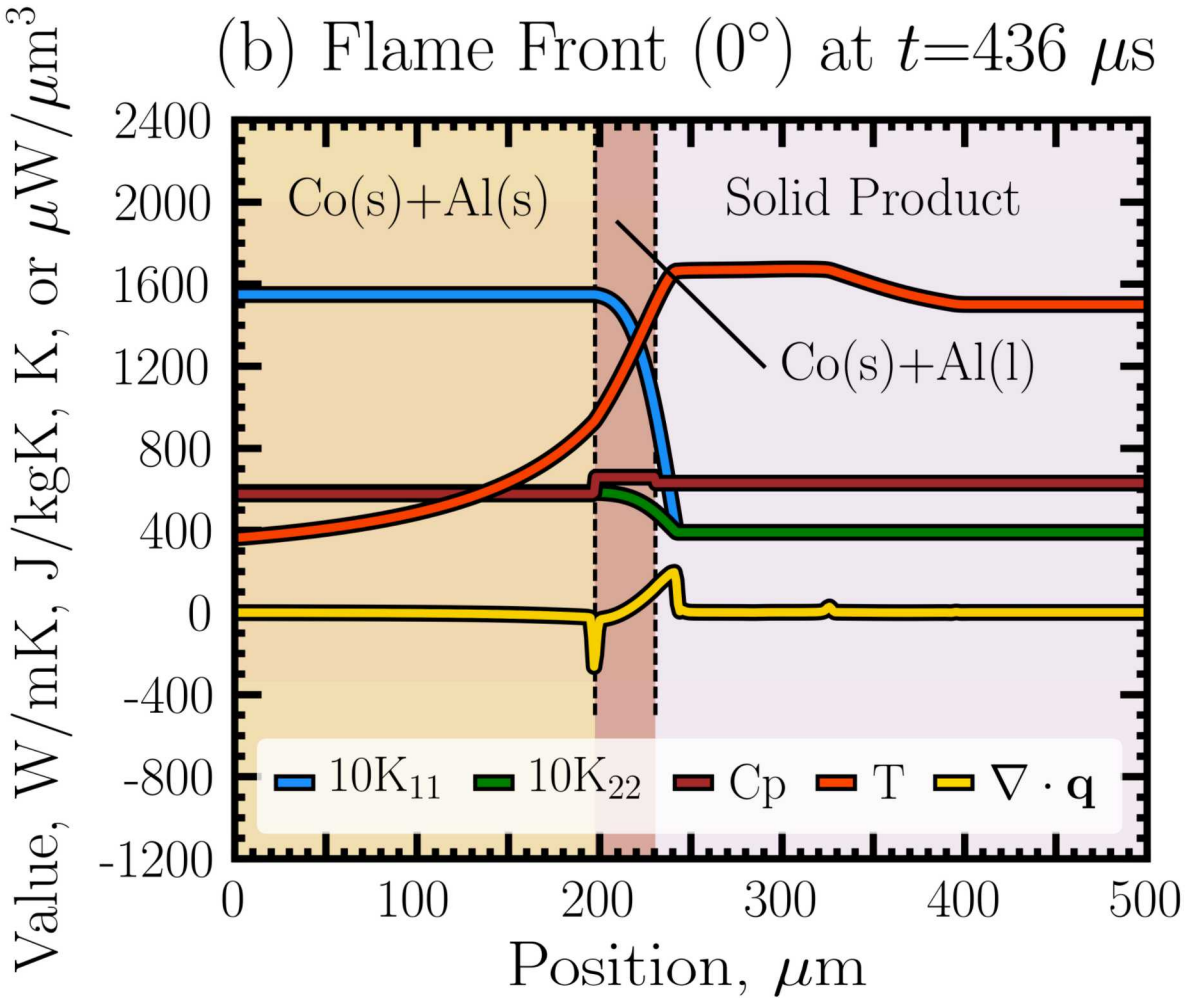

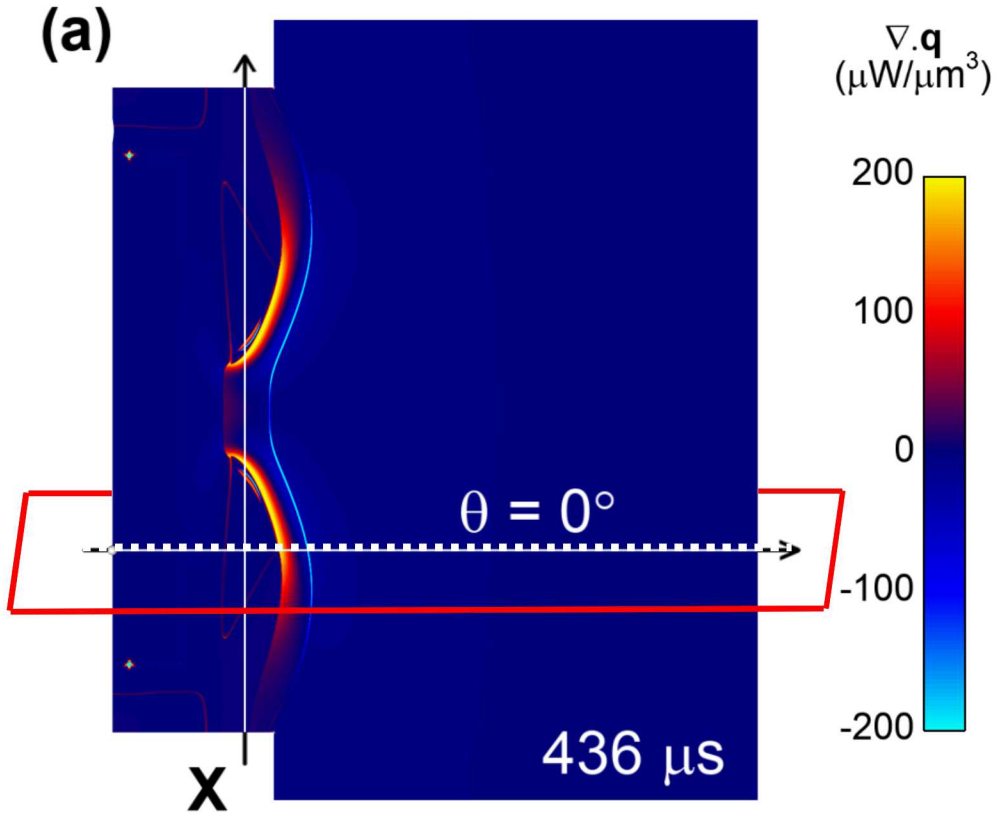

Forward flame front is *STALLED* at t = 436 μs

125 nm BL Thickness / Mode II: Spin Band Interrogation

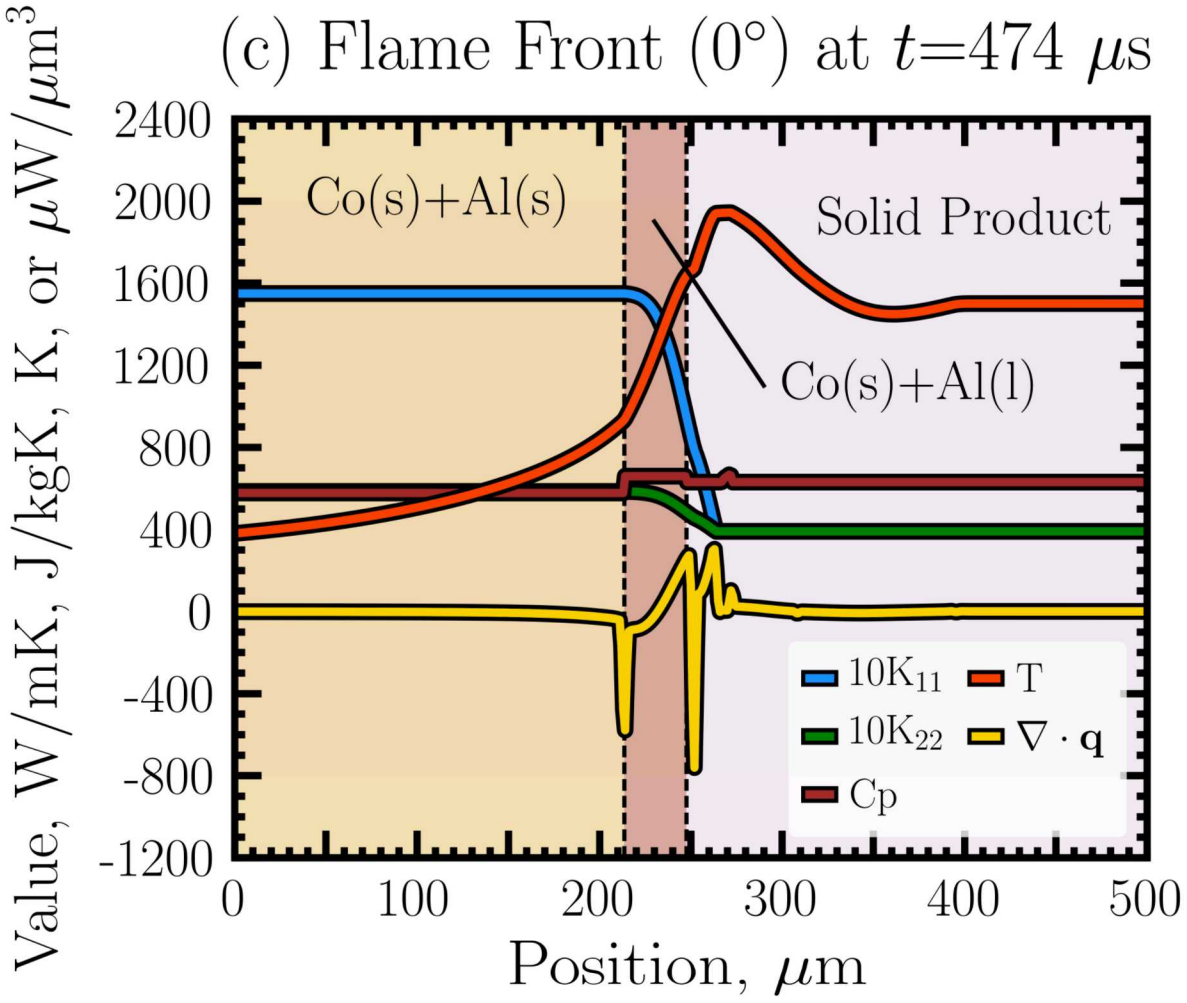

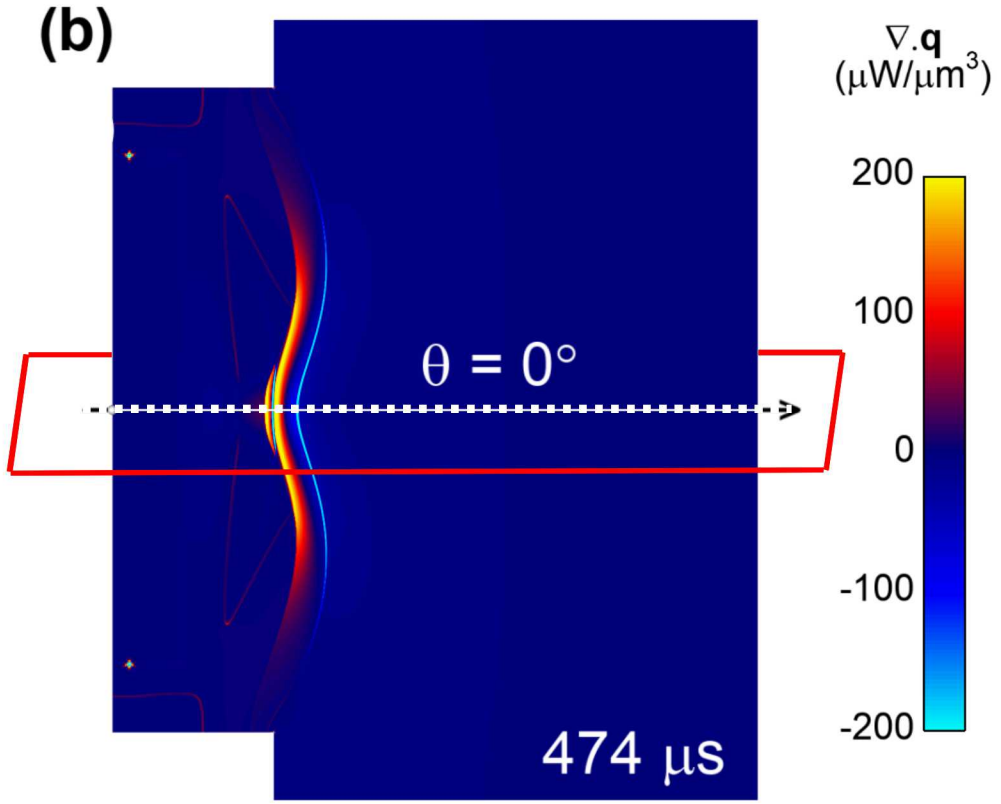

Forward flame front *AFTER* the collision; brief propagation in *NET DIRECTION*

125 nm BL Thickness / Mode II: Spin Band Interrogation

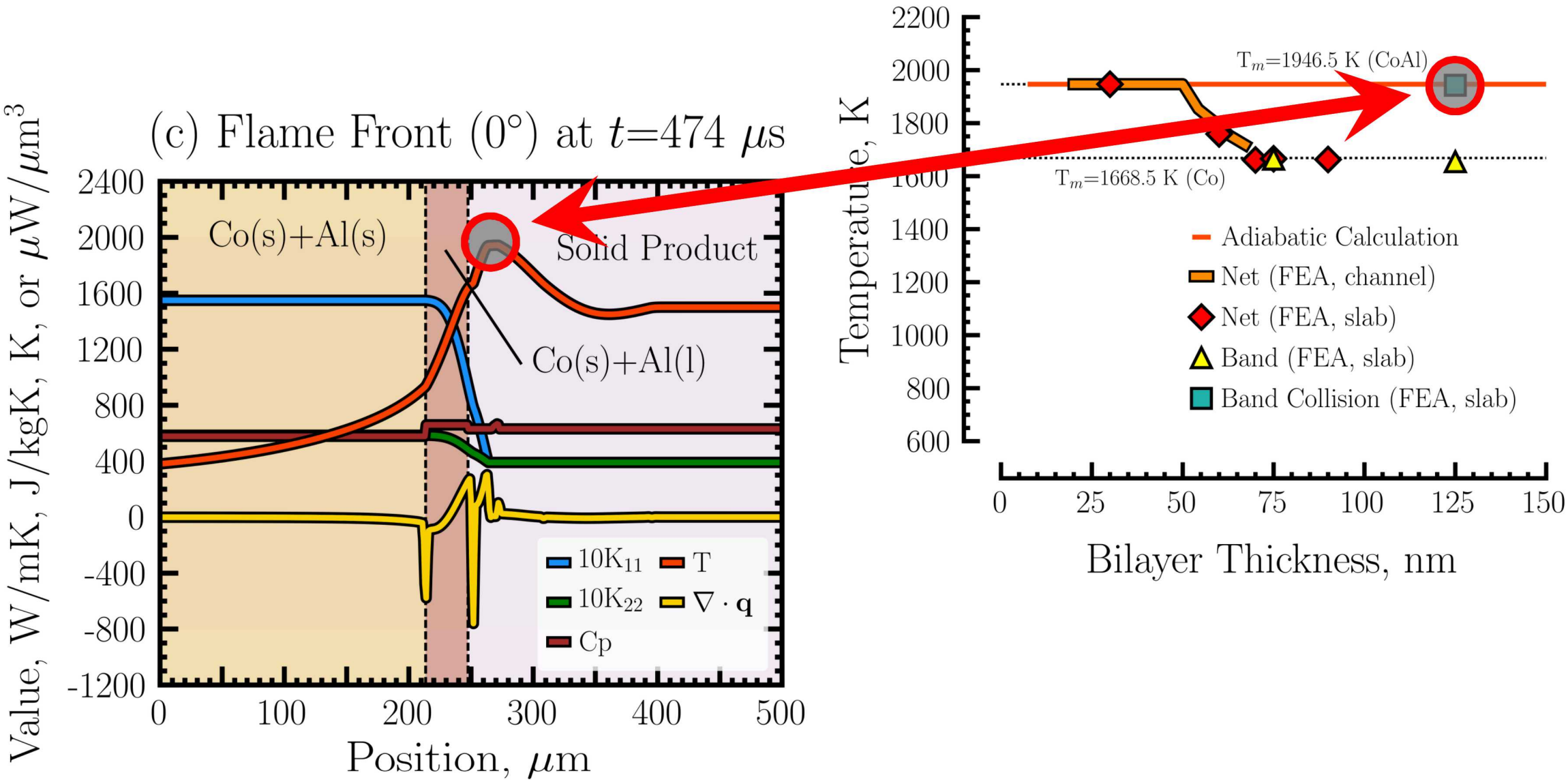

Enthalpy-Temperature Diagram (Adiabatic Flame Temperature)

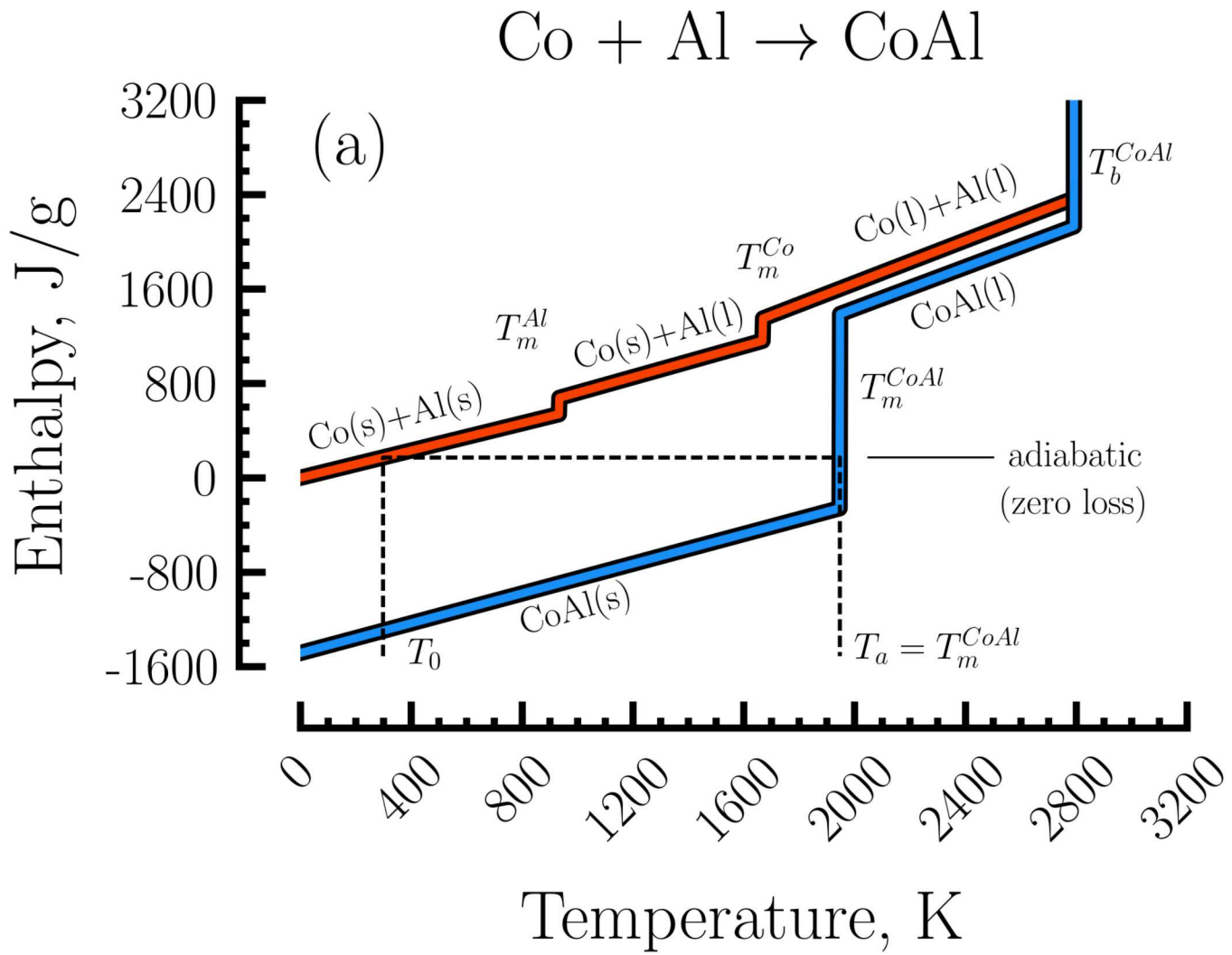

Enthalpy-Temperature Diagram (3D FEA Simulation Results)

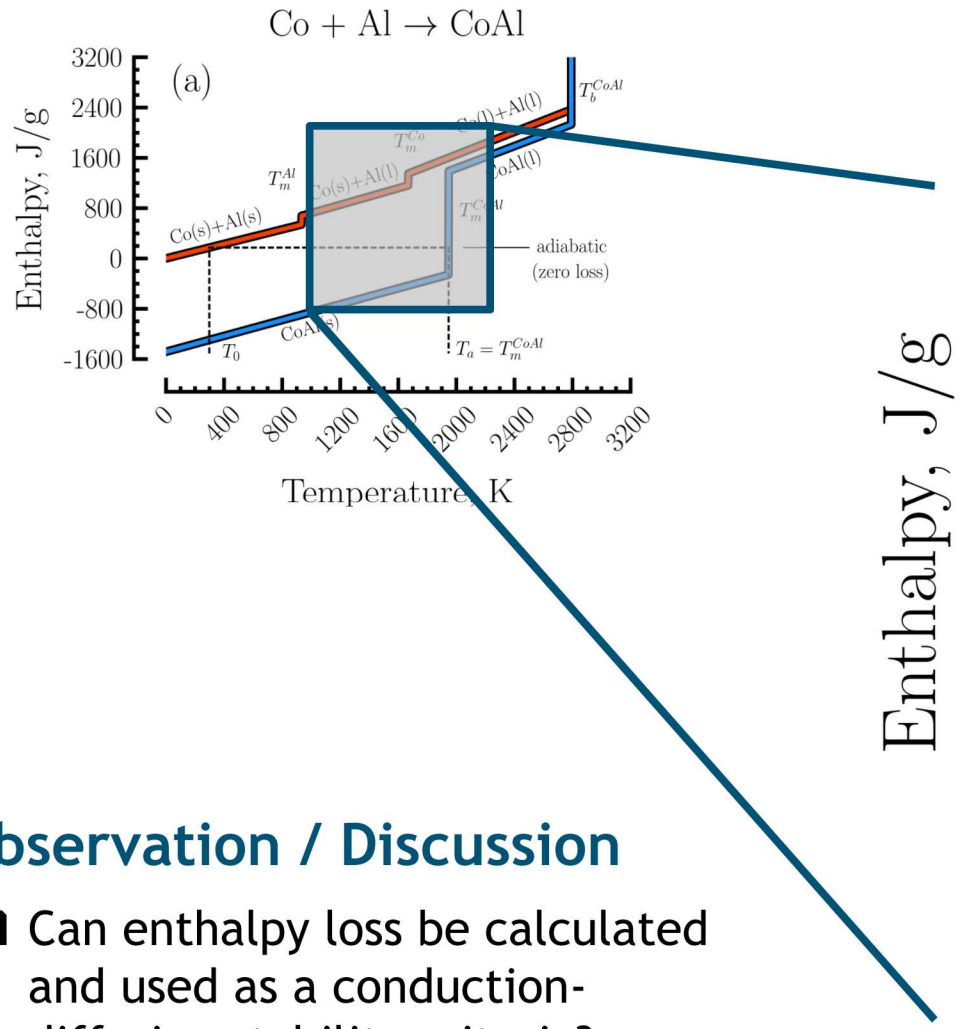

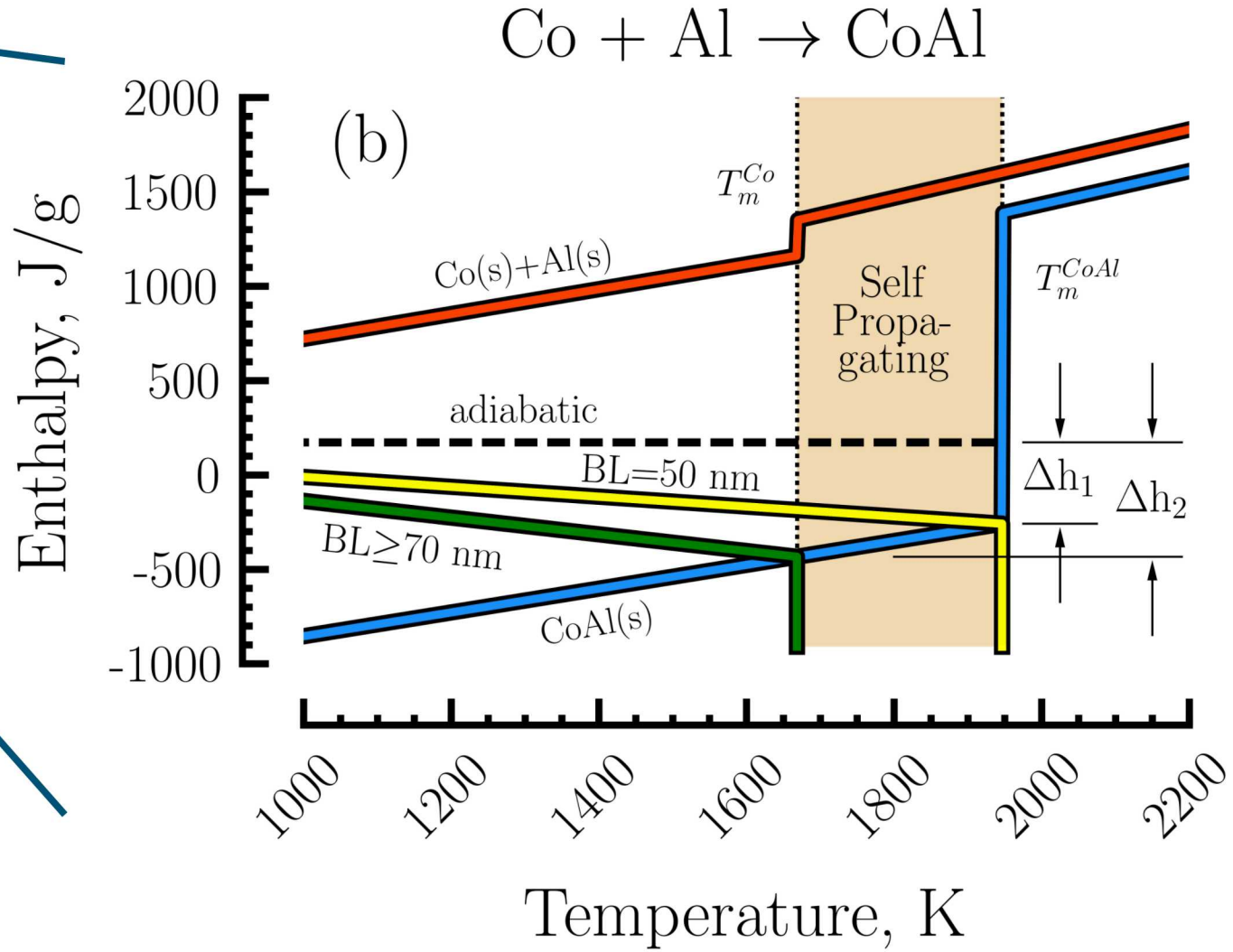

Observation / Discussion

- Can enthalpy loss be calculated and used as a conduction-diffusion stability criteria?

CONCLUSIONS

Conclusions

Empirical reduced order models enable large 3D FEA simulations

Multilayer overall geometry and edge effects influence the stability of weak and/or marginally propagating flames

- Enhanced conduction losses around corners
- Heat concentrations in thermally insulated corners

Spin bands tend to propagate into thermally (but not chemically) affect diffusion zones

- This supports Reeves and Adams (2014) hypothesized mechanism

Evidence for an enthalpy-based stability criteria with these multilayer designs

- Self-propagating reactions tend to lie between the cobalt and product melt isotherms

References

Abere, Yarrington, and Adams, "Heating rate dependent ignition of Al/Pt nanolaminates through pulsed laser irradiation," *J. Appl. Phys.*, **123**(23):235304, 2018.

Adams, "Reactive multilayers fabricated by vapor deposition: A critical review," *Thin Solid Films*, **576**:98-128, 2015.

Adams, Abere, Sobczak, and Rodriguez, "Stabilizing effects of oxidation on propagating formation reactions occurring in nanometer-scale metal multilayers," *Thin Solid Films*, **688**:137349, 2019.

Alawieh, Knio, and Weihs, "Effect of thermal properties on self-propagating fronts in reactive nanolaminates," *J. Appl. Phys.*, **110**(1):013509, 2011.

Besnoin, Cerutti, Knio, and Weihs, "Effect of reactant and product melting on self-propagating reactions in multilayer foils," *J. Appl. Phys.*, **92**(9):5474-81, 2002.

Filonenko and Vershennikov, "Mechanism of spin burning of titanium in nitrogen," *Combust., Explos., Shock Waves*, **11**(3):301-308, 1975.

Gunduz, Fadenberger, Kokonou, Rebholz, Doumanidis, and Ando, "Modeling of the self-propagating reactions of nickel and aluminum multilayered foils," *J. Appl. Phys.*, **105**(7):074903, 2009.

Hardt and Phung, "Propagation of gasless reactions in solids-I. Analytical study of exothermic intermetallic reaction rates," *Combust. Flame*, **21**(1):77-89, 1973.

Hobbs, Adams, and McDonald, "Heat transfer in reactive Co/Al nanolaminates," *Advanced Computational Methods and Experiments in Heat Transfer X*, **61**:127, 2008.

Ivleva and Merzhanov, "Three-dimensional spinning waves in the case of gas-free combustion," *Doklady Phys.*, **45**(4):136-141, 2000.

Jayaraman, Knio, Mann, and Weihs, "Numerical predictions of oscillatory combustion in reactive multilayers," *J. Appl. Phys.*, **86**(2):800-809, 1999.

Kittell, Yarrington, Hobbs, Abere, and Adams, "A diffusion-limited reaction model for self-propagating Al/Pt multilayers with quench limits," *J. Appl. Phys.*, **123**(14):145302, 2018.

McDonald, Hodges, Jones, and Adams, "Direct observation of spinlike reaction fronts in planar energetic multilayer foils," *Appl. Phys. Lett.*, **94**(3):034102, 2009.

Reeves and Adams, "Reaction instabilities in Co/Al nanolaminates due to chemical kinetics variation over micron-scales," *J. Appl. Phys.*, **115**(4):044911, 2014.

Reeves, Mukasyan, and Son, "Thermal and impact reaction initiation in Ni/Al heterogeneous reactive systems," *J. Phys. Chem. C*, **114**(35):14772-80, 2010.

Salloum and Knio "Simulations of reactive nanolaminates using reduced models: III. Ingredients for a general multidimensional framework," *Combust. Flame*, **157**(6):1154-66, 2010.

Schwendeman, Kapila, and Henshaw, "A study of detonation diffraction and failure for a model of compressible two-phase reactive flow," *Combust. Theor. Model.*, **14**(3):331-66, 2010.

Yarrington, Abere, Adams, and Hobbs, "Reactive nanolaminate pulsed-laser ignition mechanism: Modeling and experimental evidence of diffusion limited reactions," *J. Appl. Phys.*, **121**(13):134301, 2017.

Acknowledgements

I would like to thank my Co-Authors, Mike Abere and Dave Adams, for experimental leadership and data collection, project manager Sophia Lefantzi, and mentors Cole Yarrington and Mike Hobbs for help running and programming the Galerkin FEA SIERRA/Aria computer code. Thanks also to the ANSYS EnSight training staff for help with visualization and post processing.

Sandia Funding Statement

Any subjective views or opinions that might be expressed in the presentation do not necessarily represent the views of the U.S. Department of Energy or the United States Government. This work is supported by the Laboratory Directed Research and Development program at Sandia National Laboratories, a multi-mission laboratory managed and operated by National Technology and Engineering Solutions of Sandia, LLC, a wholly owned subsidiary of Honeywell International, Inc., for the U.S. Department of Energy's National Nuclear Security Administration under contract DE-NA0003525.

Thank you.
Questions?

EXTRA SLIDES – Reduced Model for Co/Al (Details)

Diffusion-Limited Reaction Model [Hardt & Phung (1973)]

Energy Equation

$$\rho C_p \frac{\partial T}{\partial t} + \nabla \cdot \boldsymbol{q} = Q\rho \frac{dF}{dt}$$

Look at these terms in greater detail

Algorithm

- Choose t_b, calculate a_0 and b_0
- Choose s_i, calculate a_i, b_i, and F_i
- Solve ODEs for s and F

Sub-Grid Model Geometry

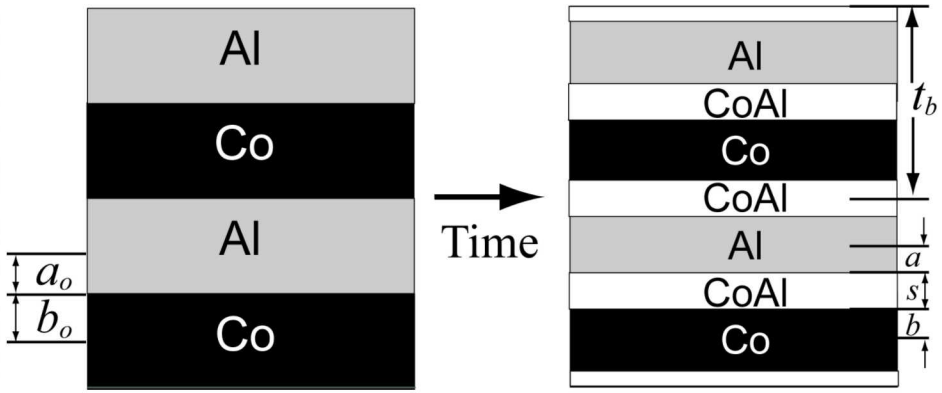

$$Co + Al \rightarrow CoAl + Q$$

ODEs

$$\frac{da}{dt} = -\frac{D}{s} \qquad \frac{ds}{dt} = \frac{D\,w}{s}$$

$$\frac{db}{dt} = -\frac{b_0}{a_0}\frac{D}{s} \qquad \frac{dF}{dt} = -\frac{D}{a_0\,s} = -\frac{D}{w\,a_0^2\,(1-F)}$$

Product Layer Thickness is

s

Bilayer Layer Thickness is

$$t_b = 2(a_0 + b_0)$$

Reacted Fraction is

$$1 - F = \frac{s}{a_0 + b_0}$$

Auxiliary Eqns.

$$r = \frac{b_0}{a_0} = \frac{\rho_{Al}\,MW_{Co}\,N_{Co}}{\rho_{Co}\,MW_{Al}\,N_{Al}} \qquad \rho = \frac{a_0\,\rho_{Al} + b_0\,\rho_{Co}}{a_0 + b_0}$$

$$a_0 = \frac{t_b}{2w} \qquad s_{max} = a_0 + b_0 \qquad b_0 = a_0\,r$$

$$a = \frac{a_0 + b_0 - s}{1 + r} \qquad b = a\,r \qquad w = 1 + r$$

Mass Fractions

$$m_{Al} = \frac{1}{1 + \frac{MW_{Co}N_{Co}}{MW_{Al}N_{Al}}} \qquad m_{Co} = 1 - m_{Al}$$

Volume Fractions

$$v_{Al} = \frac{1}{1+r} \qquad v_{Co} = 1 - v_{Al}$$

Initial Conditions

$$s_i = 5.3 \text{ nm} \qquad a_i = \frac{a_0 + b_0 - s_i}{1 + r} \qquad b_i = a_i\,r \qquad F_i = 1 - \frac{s_i}{a_0 + b_0}$$

Atom Diffusivity w/ Arrhenius-Type Diffusion Coefficient(s)

Energy Equation

$$\rho C_p \frac{\partial T}{\partial t} + \nabla \cdot \boldsymbol{q} = Q\rho \frac{dF}{dt}$$

Coupled to ODE

$$\frac{dF}{dt} = -\frac{D}{a_0\, s} = -\frac{D}{w\, {a_0}^2 (1-F)}$$

Single Arrhenius Term

$$D(T) = D_0\, exp\left(-\frac{E_a}{R\,T}\right)$$

Used by

- Mann *et al.* in *J. Appl. Phys.* (1997) ~ analytical flame model
- Hobbs *et al.* in *Comp. Method. Experim. Heat Transf. X* (2008) ~ SNL Tchem code
- Salloum & Knio in *Combust. Flame* (2010) ~ reduced reaction formalism
- Alawieh, Knio, Weihs in *J. Appl. Phys.* (2011) ~ tensor **k**
- Kittell *et al.* in *J. Appl. Phys.* (2018) ~ quench limits for Al/Pt
- And many others…

Piecewise Diffusion Coefficient w/ Temperature, Product Layer, and BL Dependencies

$$D(T,s) = \begin{cases} D_{o,0}\, exp\left(-\frac{E_{a,0}}{R\,T}\right) & \text{if } T \le T_{m,Al},\ s < s_{max} \\ D_{o,1}\, exp\left(-\frac{E_{a,1}}{R\,T}\right) & \text{if } T_{m,Al} < T \le T_{m,Co},\ s < s_{max} \\ D_{o,2}\, exp\left(-\frac{E_{a,2}}{R\,T}\right) & \text{if } T > T_{m,Co},\ s < s_{max} \end{cases}$$

$$E_{a,0} = -0.49414\, {t_b}^2 + 309.40\, t_b + 75697 \quad \text{J/mol.at.}$$

$$D_{o,0} = 1.16 \times 10^{-10} \quad \text{m}^2\text{/s}$$

Solid-Solid

$$E_{a,1} = 108000$$

$$D_{o,1} = 2.19 \times 10^{-7}$$

Solid-Liquid

$$E_{a,2} = 108000$$

$$D_{o,2} = 1.38 \times 10^{-7}$$

Liquid-Liquid

Heat of Reaction from Calorimetry

Energy Equation

$$\rho C_p \frac{\partial T}{\partial t} + \nabla \cdot \boldsymbol{q} = Q \rho \frac{dF}{dt}$$

Net Heat Release (FEA Code)

$$Q = \frac{-2H_{Rxn}}{MW_{Al} + MW_{Co}}$$ J/kg

Bilayer Dependency

Abere Empirical Fit

$$H_{Rxn}(t_b) = 46.61206 - \frac{34572440 + 46.61206}{1 + \left(\frac{t_b}{3.417932 \times 10^{-8}}\right)^{0.7584409}}$$

Kittell Q-Factor (order of one)

$$Q' = Q \times Q_f$$ *where*

$$Q_f = 1.0 + 6.6925\ exp\left(-0.04377\ t_b\right)$$

This adjustment fits the measured flame velocities, and it corrects between the actual and assumed concentration gradients

Heat of reaction is a function of the species concentration profiles (e.g., below)

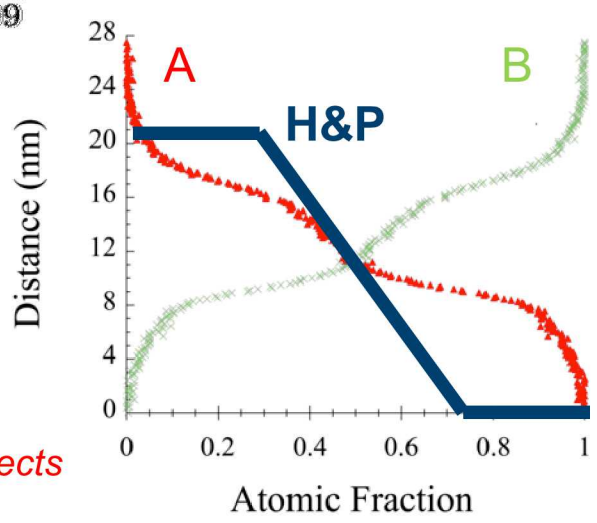

Calorimetry Data

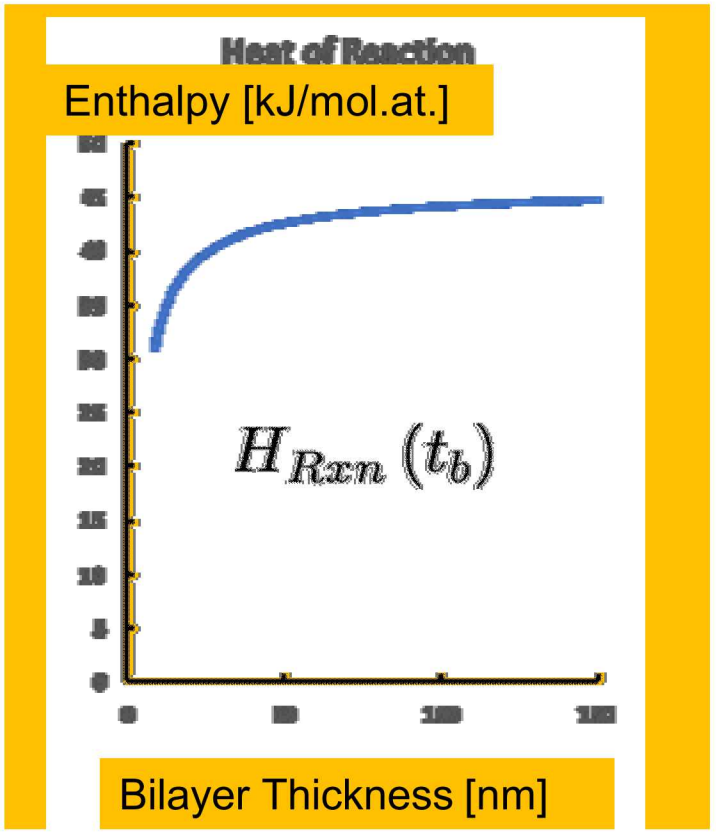

Hardt & Phung linear model geometry does not match real, sigmoidal curves

Thermophysical Properties – Thermal Conductivity

Energy Equation

$$\rho C_p \frac{\partial T}{\partial t} + \nabla \cdot \boldsymbol{q} = Q\rho \frac{dF}{dt}$$

w/ Anisotropic Tensor Conductivity

$$\boldsymbol{q} = \left\langle -k_{11}\frac{\partial T}{\partial x}, -k_{22}\frac{\partial T}{\partial y}, -k_{11}\frac{\partial T}{\partial z} \right\rangle$$

Two Directions:
In-Plane (k_{11})
Thru-Plane (k_{22})

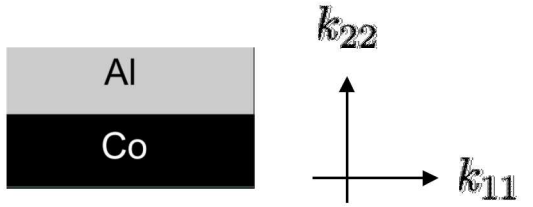

$$\nabla \cdot \boldsymbol{q} = \frac{\partial}{\partial x}\left(-k_{11}\frac{\partial T}{\partial x}\right) + \frac{\partial}{\partial y}\left(-k_{22}\frac{\partial T}{\partial y}\right) + \frac{\partial}{\partial z}\left(-k_{11}\frac{\partial T}{\partial z}\right)$$

Heat Release Rate

Kittell *et al.* in *J. Appl. Phys.* (2018) for Al/Pt Multilayers
~ "premix equals product"

$$k_{11}(T,F) = v_{Al}(F)\ k_{Al}(T) + v_{Pt}(F)\ k_{Pt}(T) + v_{AlPt}(F)\ k_{AlPt}$$

$$k_{22}(T,F) = \left[v_{Al}(F)/k_{Al}(T) + v_{Pt}(F)/k_{Pt}(T) + v_{AlPt}(F)/k_{AlPt}\right]^{-1}$$

Data Tables for k_{Al} and k_{Pt}

Single Value for k_{AlPt}

$$v_{Al} = \frac{F}{w} \qquad v_{Pt} = \frac{r\,F}{w} \qquad v_{AlPt} = 1 - F$$

Resistor Network ~ "premix is not product"

- Drives initial anisotropic values based on measured premix conductivity towards a single value for the product phase

$$k_{11,0} = c_1\ k_{Al} + c_2\ k_{Co} + c_3\ k_{mix}$$

$$k_{22,0} = \left[c_1/k_{Al} + c_2/k_{Co} + c_3/k_{mix}\right]^{-1}$$

$$k_{11}(s) = k_{11,0} + \left(\frac{k_{CoAl} - k_{11,0}}{s_{max} - s_i}\right)(s - s_i)$$

$$k_{22}(s) = k_{22,0} + \left(\frac{k_{CoAl} - k_{22,0}}{s_{max} - s_i}\right)(s - s_i)$$

Thermophysical Properties – Heat Capacity w/ Irreversible Phase Change

Energy Equation

$$\rho C_p \frac{\partial T}{\partial t} + \nabla \cdot \boldsymbol{q} = Q\rho \frac{dF}{dt}$$

Kittell *et al.* in *J. Appl. Phys.* (2018) for Al/Pt Multilayers ~ "reversible phase change"

$$C_p(T,F) = m_{Al}(F)\ C_{p,Al}(T) + m_{Pt}(F)\ C_{p,Pt}(T) + m_{AlPt}(F)\ C_{p,AlPt}$$

Data Tables for $C_{p,Al}$ and $C_{p,Pt}$

Single Value for $C_{p,AlPt}$

$$m_{Al} = \frac{\rho_{Al} F}{(\rho_{Al} + r\rho_{Pt})F + \rho_{AlPt} w (1-F)}$$

$$m_{Pt} = \frac{r\rho_{Pt} F}{(\rho_{Al} + r\rho_{Pt})F + \rho_{AlPt} w (1-F)}$$

$$m_{AlPt} = \frac{\rho_{AlPt} w (F-1)}{(\rho_{Al} + r\rho_{Pt})F + \rho_{AlPt} w (1-F)}$$

C_p model for Co/Al ~ "irreversible phase change"

- Piecewise continuous function, with constant weights and values
- Phase change via mush zones (added to C_p depending on λ)

Mush Zone (for $h_{fus,Al}$, $h_{fus,Co}$, and $h_{fus,CoAl}$)

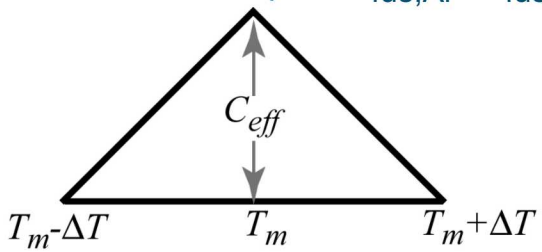

$Area = ½(base \times height)$

$h_{fus} = ½(2\Delta T \times C_{eff})$

$C_{eff} = h_{fus}/\Delta T$

$$C_p(T,s) = \begin{cases} m_{Al}C_{p,Al(s)} + m_{Co}C_{p,Co(s)} & \text{if } T \le T_{m,Al} \text{ and } \lambda < 0.5 \\ m_{Al}C_{p,Al(l)} + m_{Co}C_{p,Co(s)} & \text{if } T_{m,Al} < T \le T_{m,Co} \text{ and } \lambda < 0.5 \\ m_{Al}C_{p,Al(l)} + m_{Co}C_{p,Co(l)} & \text{if } T > T_{m,Co} \text{ and } \lambda < 0.5 \\ C_{p,CoAl(s)} & \text{if } T \le T_{m,CoAl} \text{ and } \lambda \ge 0.5 \\ C_{p,CoAl(l)} & \text{if } T > T_{m,CoAl} \text{ and } \lambda \ge 0.5 \end{cases}$$

where,

$$m_{Al} = \frac{1}{1 + \frac{MW_{Co}N_{Co}}{MW_{Al}N_{Al}}}$$

$$m_{Co} = 1 - m_{Al}$$

$$\lambda = \frac{s - s_i}{s_{max} - s_i}$$

"switching variable"

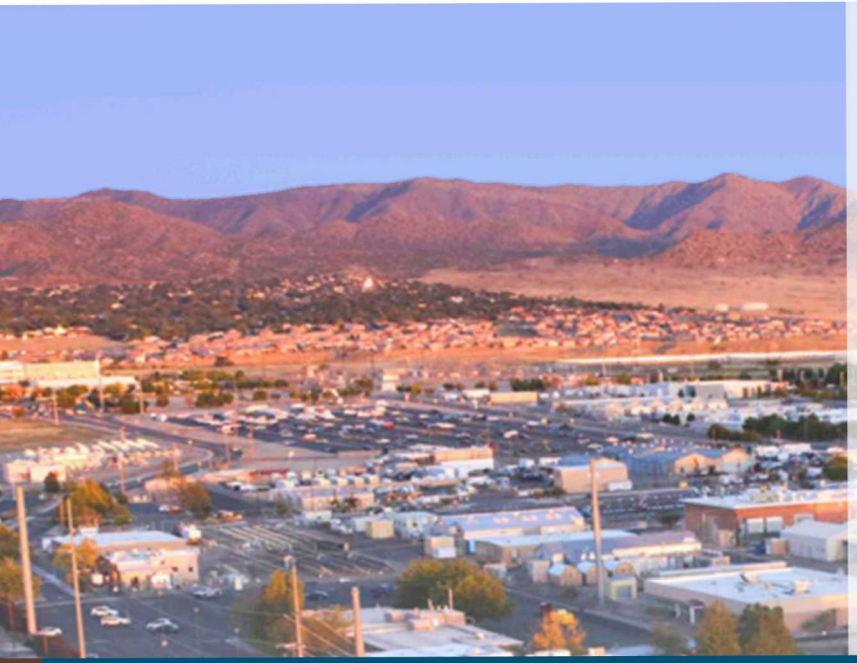

EXTRA SLIDES – Calculating the Enthalpy Losses from FEA Simulations

Calculating the Enthalpy Losses

Here's my solution, starting from the governing FEA heat equation,

$$\rho C_p \frac{\partial T}{\partial t} + \nabla \cdot \mathbf{q} = Q\rho \frac{dF}{dt}$$

FEA Heat Eqn.
(Exothermic, Q<0)

$$\rho \int_{t_i}^{t_f} \frac{\partial h}{\partial t} d\hat{t} + \int_{t_i}^{t_f} \nabla \cdot \mathbf{q} d\hat{t} = Q\rho \int_1^0 dF$$

Integrate from
reactants to products
over time
(or mass fraction)

$$\rho \left[h_{flame} - h_0\right] + \int_{t_i}^{t_f} \nabla \cdot \mathbf{q} d\hat{t} = -Q\rho$$

Evaluate what we can,
almost there

What to do with him?

Calculating the Enthalpy Losses

First, look at the heat flux vector for our 3D simulation. It is given by,

$$\mathbf{q} = \left\langle -K_{11}\frac{\partial T}{\partial x},\ -K_{22}\frac{\partial T}{\partial y},\ -K_{11}\frac{\partial T}{\partial z},\ \right\rangle$$

$$\nabla \cdot \mathbf{q} = \frac{\partial}{\partial x}\left(-K_{11}\frac{\partial T}{\partial x}\right) + \frac{\partial}{\partial y}\left(-K_{22}\frac{\partial T}{\partial y}\right) + \frac{\partial}{\partial z}\left(-K_{11}\frac{\partial T}{\partial z}\right)$$

This term is a bit complicated, but may be calculated with the post-processing software (EnSight)

When I plot $\nabla\mathbf{q}$ on the colormaps, that's what is being calculated. The heat release rate has units of [power] / [volume], e.g. micro-Watts per cubic micron. It is more like a heat flow where **positive values** are a source/exotherm and **negative values** are a sink/endotherm.

Calculating the Enthalpy Losses

Moving on, what about the time integration? We can do it in a moving frame of reference, ***if*** the function is a steady wave.

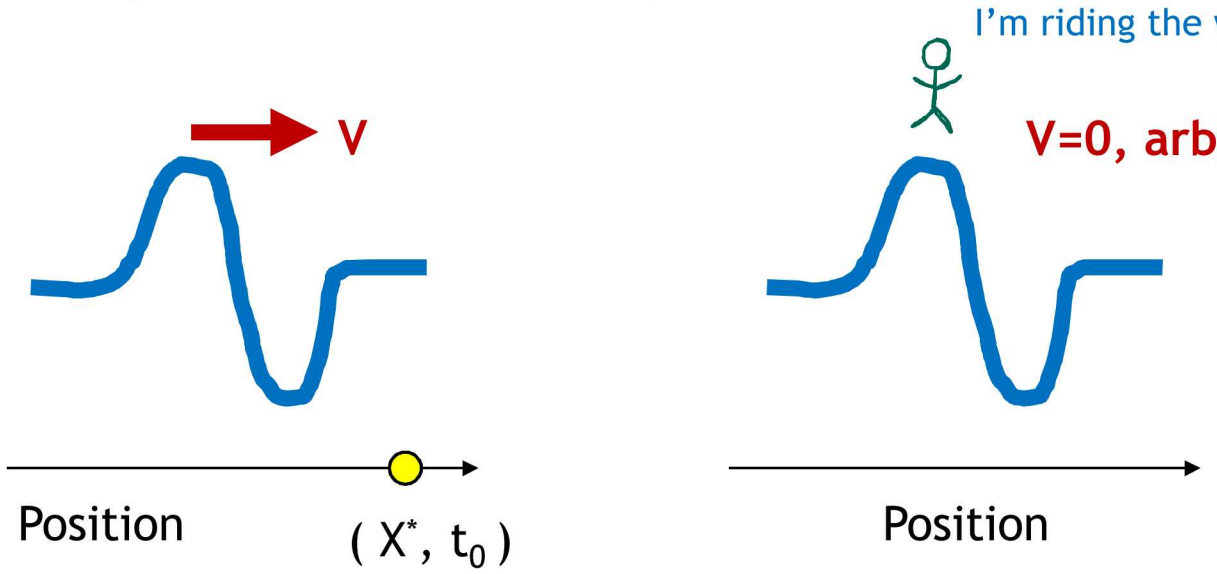

$$g(x,t) = f(x - v\,t) \rightarrow \int_{t_i}^{t_f} g(x^*,\hat{t})\; d\hat{t} = -\frac{1}{v}\int_{u_i}^{u_f} f(\hat{u})\; d\hat{u}$$

Wave Function

Integrate a mass point over time

Integrate over distance in a moving frame of reference

Calculating the Enthalpy Losses

This is the **final equation**, used to compute the enthalpy loss from the FEA simulation results. There are a lot of tricky sign conventions that have to be navigated. All the steps you need are on the previous 3 slides.

$$[h_0 - h_f] = \frac{1}{\rho v}\int_{x_f}^{x_0} \nabla \cdot \mathbf{q} d\hat{x} - \|Q\|$$

$$\left\{\begin{array}{c}\text{Enthalpy}\\ \text{Loss}\end{array}\right\} = \left\{\begin{array}{c}\text{Net Accumulation}\\ \text{of Heat in Flame}\end{array}\right\} - \left\{\begin{array}{c}\text{Heat of}\\ \text{Reaction}\end{array}\right\}$$

Notes: subscript "0" is the initial condition (i.e. T_0, x_0, t_0) and subscript "f" is in the flame (i.e. T_f, x_f, t_f). Since the volumetric heat release, Q, is negative, I put the absolute value so that you cannot get confused by the sign convention.

Calculating the Enthalpy Losses

Case i. Thermally-affected area is infinite
(i.e. huge thermal sink, zero gradient)

$$[h_0 - h_f] = \frac{1}{\rho v}\int_{x_f}^{x_0} \nabla \cdot \mathbf{q} d\hat{x} - \|Q\|$$

0

The chemical heat release does ***not*** go to raising the temperature

Case ii. Thermally-affected area is close to zero; exotherm is a delta function at the flame front

$$[h_0 - h_f] = \frac{1}{\rho v}\int_{x_f}^{x_0} \nabla \cdot \mathbf{q} d\hat{x} - \|Q\|$$

v. sharp gradient

= 0

Calculating the Enthalpy Losses

Returning to the **enthalpy-temperature diagram**, the stability criteria may be written via inequalities, based on the final equation that we derived. For **steady flames**, the net accumulation of heat must be equal or greater than the enthalpy loss to get down to the product melt elbow, i.e.

$$\frac{1}{\rho v}\int_{x_f}^{x_0} \nabla \cdot \mathbf{q} d\hat{x} \geq \|Q\| - \Delta h_1$$

And for **any self-sustained** reactions to occur, the net accumulation of heat must stay above the cobalt melt transition, i.e.

$$\frac{1}{\rho v}\int_{x_f}^{x_0} \nabla \cdot \mathbf{q} d\hat{x} \geq \|Q\| - \Delta h_2$$

So Mode I (net flame and bands) as well as Mode II bands lie between these two inequalities. However, Mode II net flames do not exist, because these BL designs fail the second inequality (but the spin bands achieve it with preheat).

Calculating the Enthalpy Losses

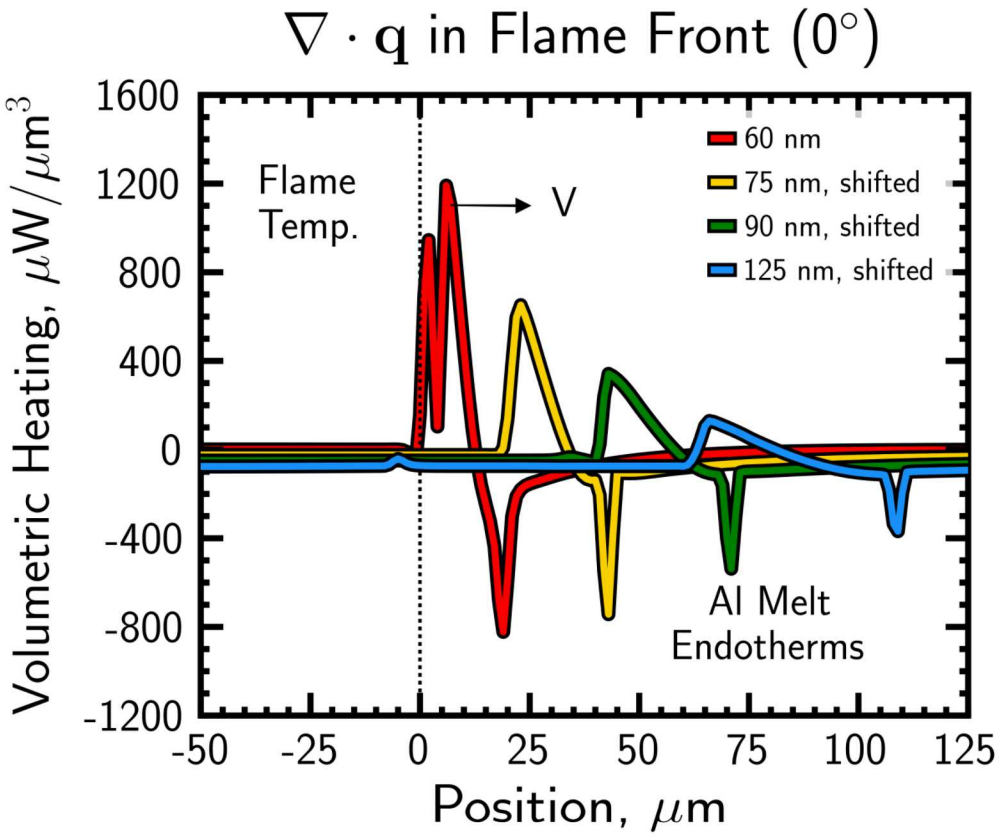

- These are the heating profiles out ahead of the leading flame; they come from the large FEA notched simulations. The exotherms are positive and the aluminum melt endotherms are negative.
- In order to use the enthalpy loss equations, we can integrate these curves from left to right. Unfortunately, these simulations do not have enough mesh resolution to get the melt endotherm exactly. So, I have been integrating the exotherms only and then subtracting the known value of the endotherm.

Calculating the Enthalpy Losses

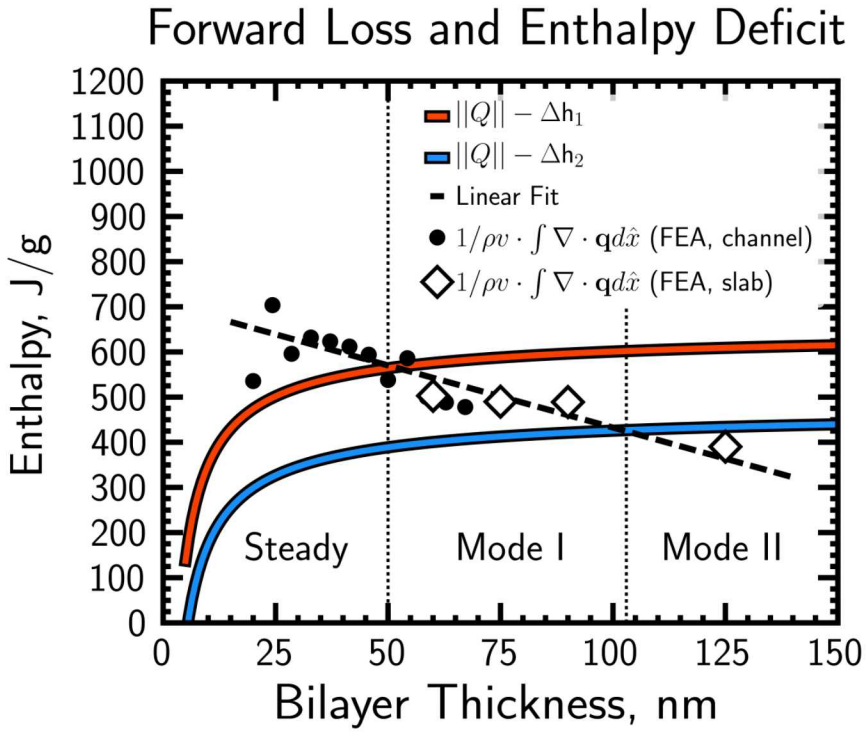

Steady flame limit

$$\frac{1}{\rho v}\int_{x_f}^{x_0} \nabla \cdot \mathbf{q} d\hat{x} \geq ||Q|| - \Delta h_1$$

Self-propagating limit

$$\frac{1}{\rho v}\int_{x_f}^{x_0} \nabla \cdot \mathbf{q} d\hat{x} \geq ||Q|| - \Delta h_2$$

See the enthalpy-temperature diagram in Fig. 12, and the derivation of the loss equation

- I calculated the net heat accumulation for a handful of FEA simulations (channels and notched slabs) but it is numerically noisy. Basically, I picked a time where I though the profile looked steady; and to make up for the numerical error I have a linear curve fit through the data.
- From this plot, I estimate that the Mode I to II transition is at 103 nm (based on the linear best fit).
- At low BL, it looks like the net heat accumulation may stay above the Mode I limit. This is very interesting, and might help explain why no evidence of spin was observed there. But still something to investigate further; I don't have enough time to fit the low BL Q-factors to complete the model description there.